POLITECNICO DI MILANO

Scuola di Ingegneria Civile, Ambientale e Territoriale
Corso di Laurea Magistrale in Ingegneria per l'Ambiente e il Territorio

GROWTH AND NUTRIENT PARTITIONING IN DECIDUOUS FRUIT TREES: A MODELLING FRAMEWORK LINKING SEASONAL AND INTER-ANNUAL DYNAMICS

Supervisor: Prof. Paco Melià
Assistant Supervisors: Dr. Daniele Bevacqua

Master Graduation Thesis by:
PIETRO SALVAGNO
Student ID: 878090

Academic Year 2018-2019

Contents

Acknowledgments

Questa tesi non sarebbe stata possibile senza la competenza e l'entusiasmo di Daniele Bevacqua, che mi ha prima coinvolto e poi aiutato quotidianamente durante tutta la permanenza ad Avignone. Grazie di cuore.
Grazie anche al mio relatore, prof. Paco Melià, che mi ha seguito nelle ultime fasi del lavoro con pazienza e dedizione.
Ringrazio particolarmente tutte le persone che ho conosciuto in Francia, come Marta, Matteo, Dario ed Enrico, che mi hanno accolto senza esitazioni e con cui ho coltivato splendide amicizie. Avete reso questa esperienza unica e indimenticabile.

La mia famiglia, i miei genitori e mio fratello Matteo hanno vissuto con me tutte le difficoltà, tutta la fatica, eppure anche tutte le grandi soddisfazioni che ho provato durante questi anni al Politecnico, un percorso di cui questo lavoro è conclusione e apice: a loro, e a loro soltanto, è interamente dedicato, come prova tangibile di quanto sia stato importante avere la loro fiducia e il loro supporto.

Un grazie sincero e profondo a Fede, che ha addolcito gli ultimi anni di università e che continuerà per sempre ad essere la mia fonte di ispirazione e di gioia. Nessun'altra colazione sarà più come prima.
Come non ringraziare Gaia, in cui ho trovato contempornaeamente una grande amica e una grande maestra. Quasi mi dispiace sapere che non

avremo più niente da studiare insieme.
Grazie a tutti i compagni che ho conosciuto a lezione e che, come me, capiscono cosa vuol dire raggiungere questo traguardo.

Davvero grazie a tutti i miei vecchi coinquilini di Milano, Gio, Fra e Mati, con cui ho creato legami profondi e con cui ho scoperto e coltivato vere passioni. Non c'è bisogno di sottolineare quanto ci siamo divertiti in questi ultimi anni.

I miei amici di sempre, di una vita, si meritano il più caloroso dei ringraziamenti e degli abbracci: Frigge, Fillo, Marghe, EdoL, EdoB, Virgi, Gotte, Pippi, Gaia, Marra, Berto, Fra, Pippo, Nino; insieme siamo cresciuti, e insieme continueremo a crescere.

Infine, una riconoscenza speciale a tutti i membri, vecchi e nuovi, del team ChaseCake. Con voi ho condiviso vittorie e, soprattutto, tante sconfitte.

Cya in da Nexus!

Abstract

In plant science, a gap exists between empirical models, aimed to evaluate in a quantitative way the productivity of crops, and mechanistic models, aimed to provide an interpretation of general physiological processes. In this thesis we tried to integrate the two approaches in order to describe the developmental dynamics of a deciduous fruit tree, including the vegetative growth and the production of fruits as well.

First, we analyzed data from an experimental peach orchard, to derive general morphometric relationships between measurable variables, such as shoot length and fruit diameter, and the biomass of the different plant organs necessary for the subsequent development of the model.

Building upon the pioneering work of Thornley (1998), who proposed a general model of vegetative growth and nutrient partitioning in plants, we developed a model incorporating the main aspects that could make it able to reproduce not only the seasonal changes on the allocation of resources but also the fruit size and abundance dynamics. Following theoretical sources and simple physical knowledge, we translated the reasons behind fruits drop in mathematical terms, choosing the best relation among a set of candidates via a model selection based on the Akaike Information Criterion. Then, we calibrated the overall model describing the dynamics of a deciduous fruit tree and we applied it to the case study of the peach tree. The model could realistically explain data collected in 2013, in particular average shoot length and shoot abundance, average fruit diameter and fruit abundance.

We finally tried to overcome the historical limit of this kind of models to be restricted to a single growth season. We identified empirical relationships linking the total shoot length at the end of the growth season with the number and the size of new shoots and new fruits at the beginning of the following year, thus implementing a time-discrete model summarizing the phenological phase of dormancy. This multiannual version of the model was calibrated against data from the transition between years 2012 and 2013 and between 2013 and 2014, and validated against data from years 2014 and 2015. The model was unfortunately not able to reproduce our observations with sufficient precision: we thus point out the necessity of understanding and including the nutrient storage processes of the tree over subsequent seasons.

Sommario

In botanica esiste un'inconciliabilità tra modelli empirici, che forniscono valutazioni quantitative di produzione di frutta, e modelli meccanicistici, che interpretano la fisiologia generale delle piante. In questa tesi si propone un modello che integri i due approcci allo scopo di riuscire a descrivere tutti i processi coinvolti nello sviluppo di un albero da frutta stagionale, compresa la crescita vegetale così come la riproduzione.

Prima di tutto, vengono analizzati dati ricavati da un frutteto sperimentale di peschi per derivare relazioni morfometriche generali tra le variabili misurabili, come la lunghezza dei nuovi rami o il diametro dei frutti, e la biomassa dei diversi organi della pianta, necessaria successivamente per lo sviluppo del modello.

Adottando come punto di partenza il pionieristico lavoro di Thornley (1998), che presentò un modello generico di crescita vegetale e partizione di nutrienti nelle piante, abbiamo svilluppato un nuovo modello aggiungendo tutte le caratteristiche per renderlo capace di riprodurre non solo i diversi regimi stagionali di allocazione delle risorse ma anche le dinamiche di massa e abbondanza della frutta prodotta: ispirandoci a fondamenti teorici e semplici meccanismi fisici, si traducono in termini matematici le ragioni che provocano la caduta dei frutti e si seleziona, tra più relazioni candidate, quella che meglio descrive il fenomeno, ricorrendo a un metodo di selezione di modelli basato sull' Akaike Information Criterion.

Quindi, il modello viene calibrato e applicato al caso di studio del pesco. I

risultati hanno ricalcato realisticamente le osservazioni riportate durante la stagione dell'anno 2013, in particolare quelle relative a lunghezza media e abbondanza dei nuovi rami, a diametro medio e abbondanza dei frutti.
Infine è stato tentato di superare il tradizionale limite di questo genere di modelli, ovvero di concentrarsi su una singola stagione di crescita, derivando le relazioni empiriche che legano la lunghezza totale dei rami alla fine della stagione di crescita con l'abbondanza e la taglia dei nuovi rami e dei nuovi frutti dell'anno seguente, e in tal modo implementando un sottomodello tempo-discreto che riassumesse i processi che hanno luogo durante il periodo di dormienza invernale. Questa versione multiannuale del modello è stata calibrata con le osservazioni tra gli anni 2012-2013 e 2013-2014, e successivamente validata con le osservazioni delle stagioni 2014 e 2015. Sfortunatamente il modello non è stato in grado di riprodurne le dinamiche con sufficiente precisione: viene allora sottolineata la necessità di meglio comprendere e implementare i processi di accumulo e conservazione di risorse interne all'albero nel corso di più anni.

Chapter 1

Introduction and background

Plant modeling has always had a wide range of studies and applications, from forest population dynamics for environmental management to crop production and harvesting optimization, from pest control and fertilization to climate change simulations and analysis.

Among those regarding agriculture, models describing fruit tree yield in particular play a major role. In this context, a huge variety of models can be recognized, led by different principles and approaches. Some of them are focused on the growth dynamics of the fruits, which ultimately determine the final yield, having more pragmatic purposes and thus usually required to be extremely precise in quantifying the outcome of the production; for this reason they tend to simplify if not to neglect at all the description of the processes of the plant and to adopt complex and empirical mathematical equations (Grossman and DeJong 1995; Génard et al. 1998; Fishman and Génard 1998). This descriptive approach performs well within the range of the collected observations and it could have useful practical application, however it does not take into account the physiological responses of the plant to different agricultural practices or to different climatic conditions.

On the other hand, another group of models have been developed during the last decades aiming to reproduce the growth processes of the plant as

a whole, typically describing the assimilation and the allocation of carbon into different main organs (shoots and roots); this mechanistic approach can better explore the functioning of the entire plant even outside the boundaries of data, test theoretical hypotheses, or be more versatile in simulating different scenarios involving changes in both intrinsic or extrinsic conditions. Belonging to this group of models, the one of Thornley in its final version (1998) can be taken as a main example: it couples two structural components of the plant, shoots and roots, with two main substances such as carbon and nitrogen using very simple equations to describe not only their assimilation and allocation, but also their transport upward or downward through the plant body. Involving nitrogen as a nutrient is especially important because it is often considered a limiting factor for the growth (Schulze et al. 2005), despite being neglected in most studies; in addiction to that, the model seems to be able to realistically represent the behaviour of the plant and to reach the optimal shoot-root ratio even when the natural conditions are altered by the human action. Modelling different agricultural practices can be done either by modifying some of the parameters or by acting on the value of the variables themselves.

As other similar examples of this kind though, this model brings a good conceptual framework of the physiological phenomenon behind plant growth at the expense of precision and disregarding any explicit consideration about crop production.

Both the approaches presented above have limits that cannot allow us to consider the nutrient partitioning towards all the compartments of a deciduous fruit tree at the same time, preventing the description of how different inputs influence the fruit yield in the short and in the long term. We focused our work on creating a model that could meet these needs.

1.1 The case study

Fruit trees are one of the main type of crop in agriculture, and most of them are perennial deciduous woody plants. This means that they can live for many years if not for decades, but they are subject to a complex annual cycle involving many phenological events: early in summer, an active vegetative and reproductive growth is kept until the arrival of autumn, when the tree starts to prepare itself for the cold months ahead. During winter, it enters a period of growth cessation and slow metabolic activity, called dormancy, which stops when spring comes and temperatures rise again; the tree can then fuel the growth processes again and a new annual cycle begins (see Figure 1.1).

With dormancy triggered presumably by a combination of photoperiod and temperature changes, the tree stops its vegetative production in order to protect its growing cells from the incoming weather. Doing so, it has a short time window in which its leaves are still performing photosynthesis, but no resource is allocated to the development of organs: photosynthates in excess are not wasted, instead they are stored as reserves in various compartments of the plant's body (roots, trunk, branches, buds).
Months later, when the new growth season has started, reserves are used as a source of nutrients to fuel the bud burst of both new shoots and flowers while new leaves are still to develop and photosynthesis has not started yet (Singh et al. 2017).

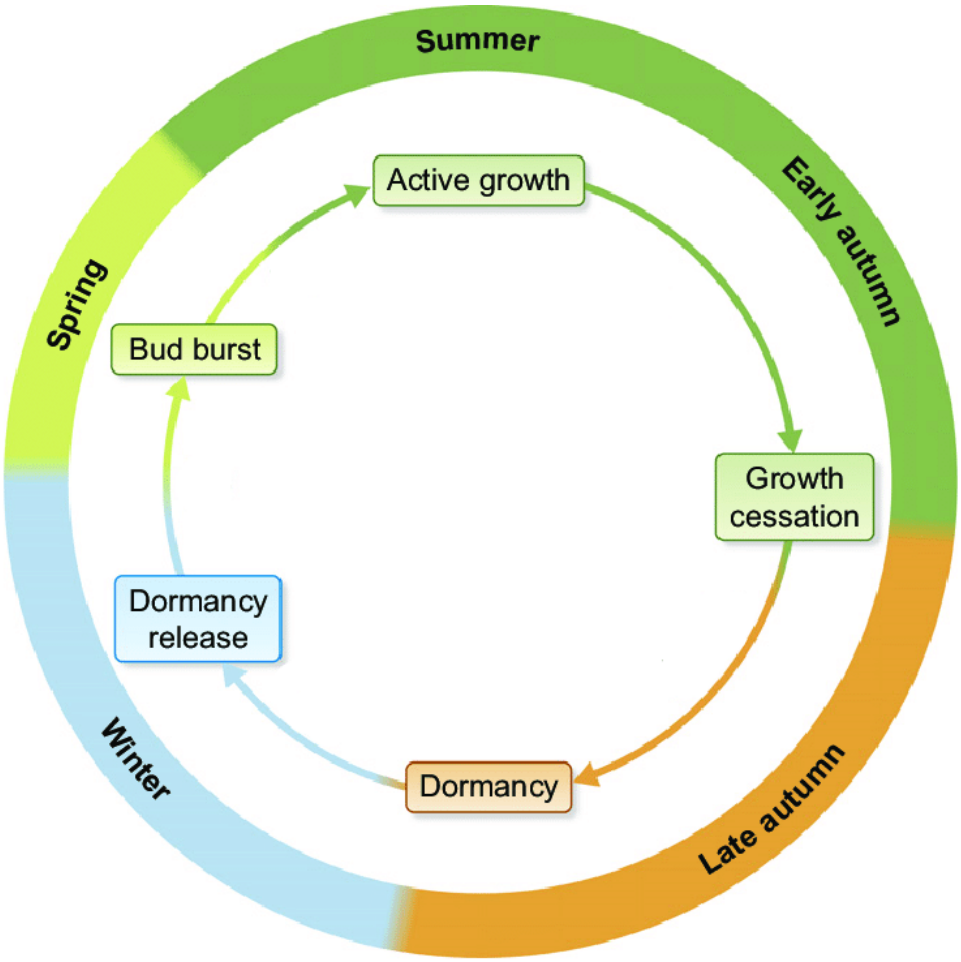

Figure 1.1: Phenological events of a deciduous fruit tree (Singh et al. 2017).

Most deciduous fruit trees share the same structure, which includes an aerial part composed by shoots and leaves performing photosynthesis and thus assimilating carbon; an underground part formed just by roots, with the role of absorbing water and nutrients from the soil (nitrogen, phosphorus, etc.); and then a woody compartment connecting the previous two, referred to as the trunk, through which substances are exchanged and transported. The trunk is mostly identifiable as a dead tissue, the heartwood, and an external living tissue, the so called sapwood. The sapwood is crossed by two different vascular vessels: the phloem (where sugars and nutrients are carried) and the xylem (transporting mainly water): using a dead non-respiring biomass as the supporting apparatus, the functional limitation of the size of the vegetative body no longer applies, removing the limitations to growth to plants that do not lignify (Schulze et al. 2005).

Being the third economically important global tree crop within the *Rosacee* family, understanding the growth dynamics of *Prunus persica* (L.) Batsch, or peach as it is called commonly, is one of the main research subjects of the French National Institute of Agricultural Research (INRA). The institute has an active collaboration with Politecnico di Milano: it provided us the data to adopt the peach tree as a case study, and supported us during a six-month internship in Avignon.
Peach trees are structured in a wooden body from which roots descend into the underground and above which old branches develop. At the end of the growth season, buds are generated along the one-year-old shoots, blooming at the beginning of the next season into new vegetative shoots or into new reproductive organs, i.e. single pink flowers, eventually becoming new fruits after impollination. The shoots, once developed after the summer growth, will become the structure along which new buds will form, so closing the cycle.

Knowing the principles just presented, peach farmers are encouraged to perform two main types of agricultural practices to influence and to increase the total final yield: the first one is the thinning, meaning the removal of some of the fruits in order to reach an optimal leaf area/fruit ratio and thus to decrease competition among fruits themselves. Indeed, if the thinning is performed in the early stages of the fruit development, the plant can allocate its limited resources to a minor number of fruits and the farmer is likely to obtain a smaller quantity of them with a larger size though, satisfying current commercial requirements.

The second main practice is called pruning, defined as the cut of one-year old-shoots right before the end of the dormancy period. As a consequence, vegetative growth is enhanced during the following season and at the end of it more shoots will be old enough to bear both new vegetative and reproductive buds. The purpose of pruning is therefore to increase the overall yield of the plant in the year after it is performed and in the long run, temporary decreasing plant productivity during the year in which the practice is carried out.

Figure 1.2: Example of peach tree branches of different age. One-year-old shoots are those bearing new shoots and flowers, whose buds are already broken.

1.2 Aims and structure of the thesis

The main purpose of this thesis is to fill the gap between the different approaches presented above, overcoming their reciprocal limitations in order to converge into a new model based on mechanistic processes but, at the same time, being able to accurately reproduce the behaviour of a generic deciduous fruit tree and to describe quantitatively its fruit production during several years.

We declined this goal into: (a) writing the mathematical relationships that can describe fruit growth, size and abundance over time; (b) modifying Thornley's model (1998) to adapt it to deciduous fruit trees, adopting and including all the aspects regarding their physiological processes and their reproductive patterns; (c) calibrating the model for our case study, the peach tree, using the available data to asses its quality and precision; (d) expanding the capacity of the calibrated model to describe a single growth season

into several sequential seasons instead, thus taking into account how the dormancy influences the plant's phenological cycle.

We structured the present work accordingly to the goals listed above. Chapter 2 presents the available data collected at INRA, their analysis and the morphometric relationships we derived in order to make the measurements usable in the future model. Chapter 3 describes in details Thornley's original model on which this thesis is based, it explains both the mathematical and the mechanistic aspects of the equation system, later presenting how we introduced our modifications following which theoretical knowledge and hypotheses. Chapter 4 describes all the calibrations needed to apply our new modified model to the specific peach tree, first with an offline procedure to find the parameters regulating fruit abundance over time and then with an online calibration to calibrate eventually the net rate of photosynthesis and the plant efficiency in converting non structural carbon into new fruit biomass. Chapter 5 shows the steps made towards a multiannual model, how we managed to summarize the changes between the dormancy period and the growth season to make the system able to run over several years with the minimum number of external inputs needed. Finally, Chapter 6 concludes the thesis discussing the main results obtained from simulations, evaluating the overall quality of the model and its further possible improvements and developments.

Chapter 2

Available data

During the growing seasons of 2013 and 2014, an experimental peach orchard of 17 late-maturing trees (cultivar Suncrest/GF677), planted in 1998 at the INRA Centre of Avignon, was monitored on a weekly basis to collect several type of measurements regarding growth over time, expressed here in Julian Days (JD) computed from the 1st of January. We present these measurements in form of boxplots, with every box related to a single sampling date and based on all the trees available.

Vegetative growth was observed by monitoring shoot abundance n_{sh} (considered constant after bloom onset, see Table 2.1) coupled with average shoot length l_{sh}, starting from bud burst which occurred at the beginning of April. As we mentioned in Chapter 1, records stop a few weeks after the trees no longer develop their shoots: in Figures 2.1 and 2.2 it can be noticed that, despite the high variability of the samplings, starting from measurements collected on day 175 (end of June) the growth of the shoots slows down considerably and then it stops within the last data recorded.

Tree id	n_{sh} 2013	n_{sh} 2014
1	813	699
2	4776	3772
3	1985	1737
5	396	1173
6	3138	3246
7	4738	2497
8	1488	727
9	2295	3613
10	4361	3309
11	6024	7433
12	3412	2205
13	760	627
15	2526	3568
17	2171	3455
18	5632	2921
19	1127	1119
20	2415	4379

Table 2.1: Number of shoot set by tree.

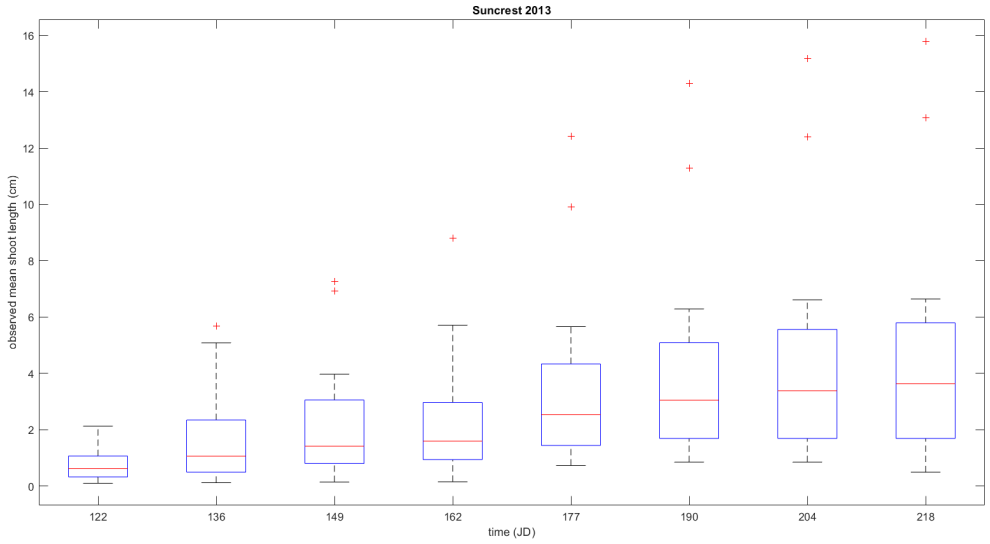

Figure 2.1: Average shoot length over time, cv. Suncrest, 2013.

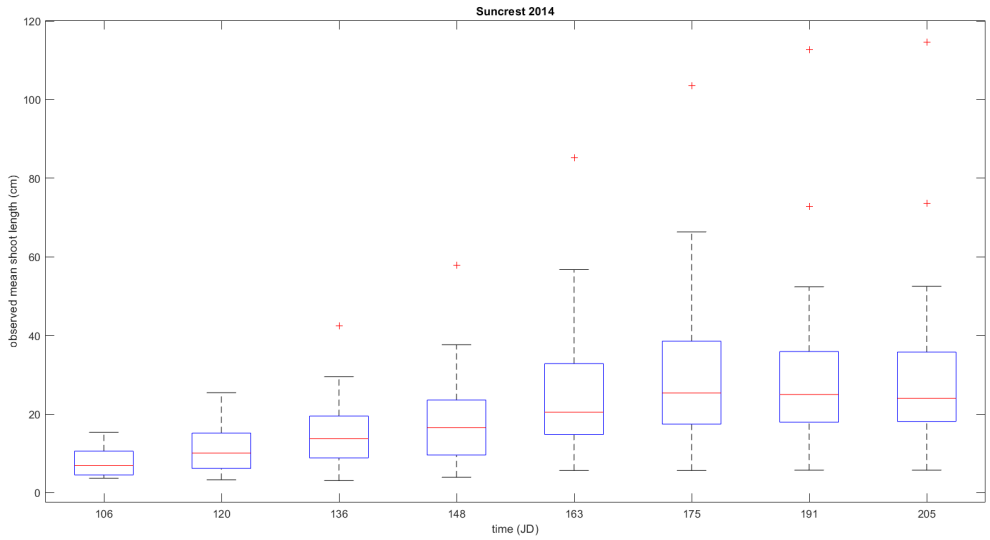

Figure 2.2: Average shoot length over time, cv. Suncrest, 2014.

Reproductive growth was measured as total number of fruits n_f (Figures 2.3, 2.4) and as the average diameter d of a single fruit (Figures 2.5, 2.6). We visually differentiated observations of trees subjected to thinning treatments, that were made on the 23rd of May in 2013 (143 JD) and on the 12th of May in 2014 (132 JD). Fruit abundance obviously drops in observations computed right after these dates, in case of thinned trees.

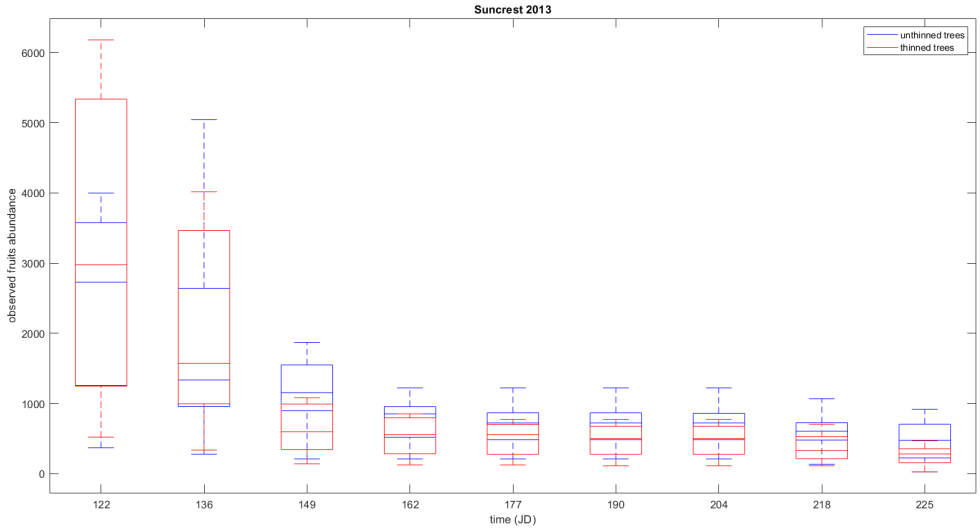

Figure 2.3: Fruit abundance over time, cv. Suncrest, 2013.

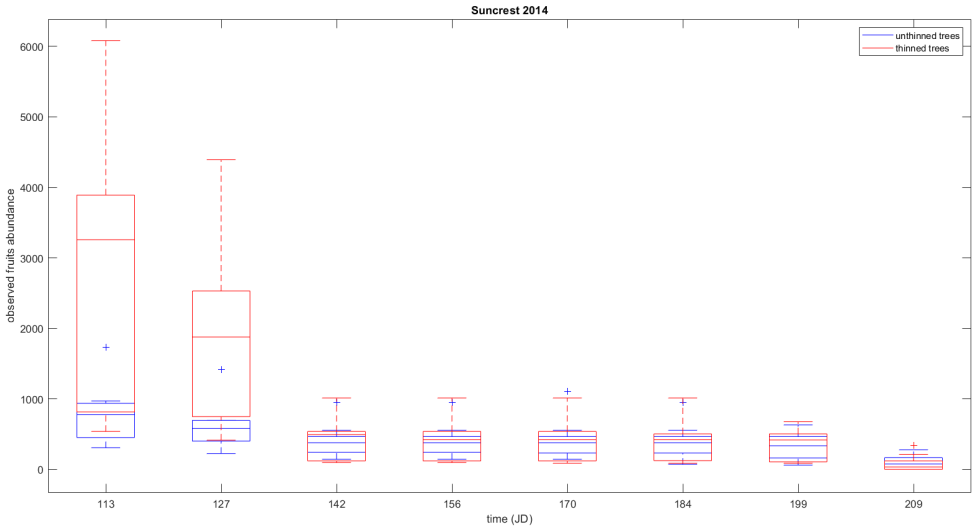

Figure 2.4: Fruit abundance over time, cv. Suncrest, 2014.

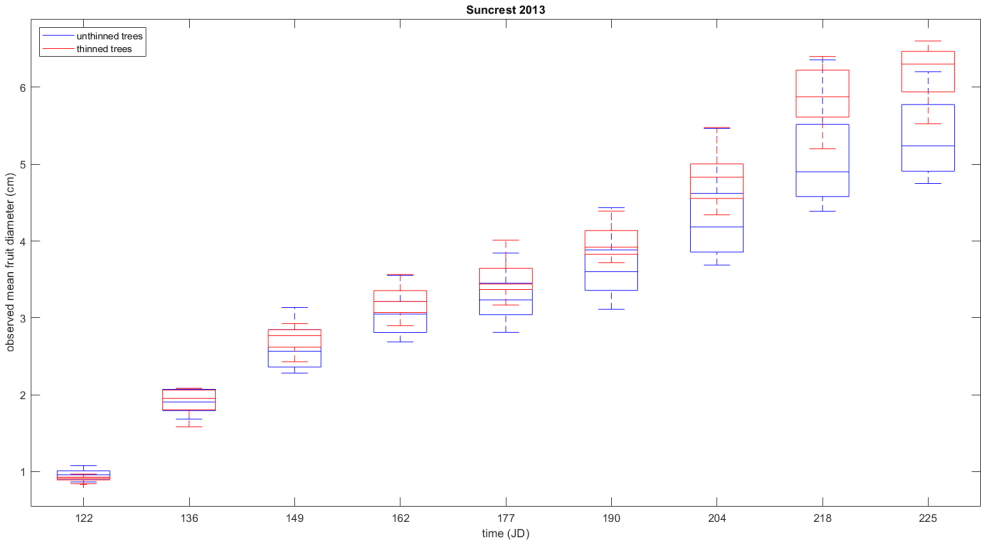

Figure 2.5: Average fruit diameter d over time, cv. Suncrest, 2013.

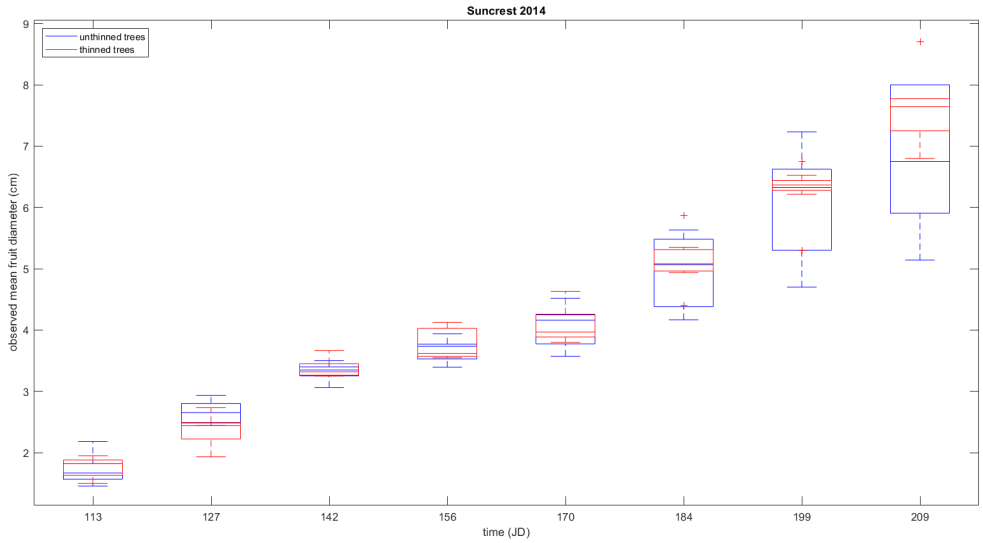

Figure 2.6: Average fruit diameter d over time, cv. Suncrest, 2014.

A last set of observations was collected at the end of the growing season of 2015 from the same orchard: the final sum of the length of all the shoots S, the final average fresh weight of fruits f, the final fruit abundance n_f (Table 2.3).

Tree id	$\boldsymbol{S(m)}$	$\boldsymbol{f(gFW)}$	$\boldsymbol{n_f}$
1	211.99	216	62
2	110.63	122	617
3	74.78	138	260
5	233.85	226	65
6	162.41	148	388
7	100.73	144	432
8	185.91	190	108
9	174.65	142	204
10	123.84	132	603
11	52.21	106	1179
12	17.94	106	692
13	153.31	144	515
15	192.61	156	597
17	196.56	148	381
18	152.51	126	625
19	32.10	100	620
20	217.89	148	334

Table 2.2: Measurements collected at the end of the growing season of 2015.

Fruit-related data were also collected from 18 trees of another peach orchard of a different type of cultivar (Magic) during the growing seasons of 2014 and 2015. Instead of collecting data from the trees as a whole, subsamples from respectively 5 and 10 representative shoots were taken for each tree; it also must be said that some observation was cut off, especially in 2014, due to disease infections altering the natural abundance and growth of fruits. Data are box-plotted in Figures 2.7, 2.8, 2.9, 2.10.

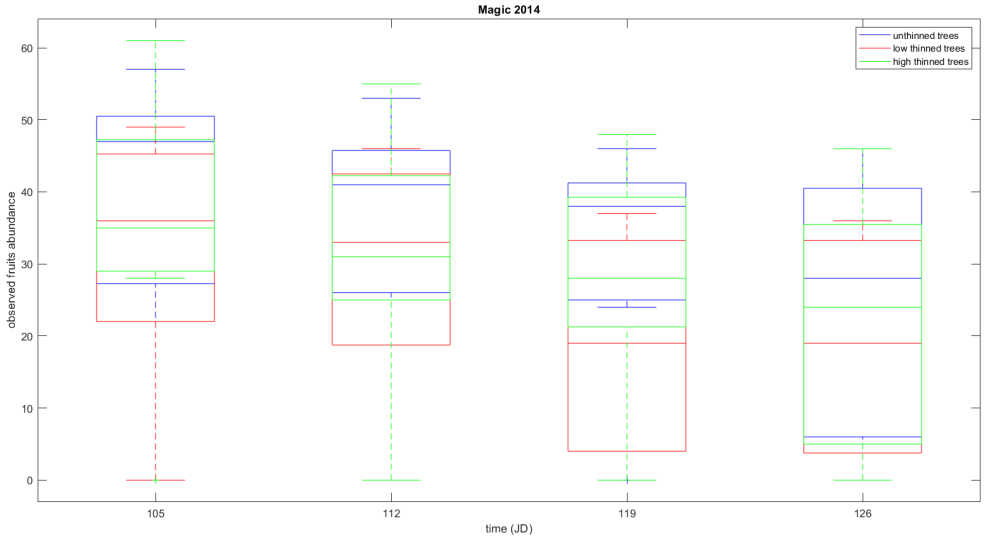

Figure 2.7: Fruit abundance over time, cv. Magic, 2014.

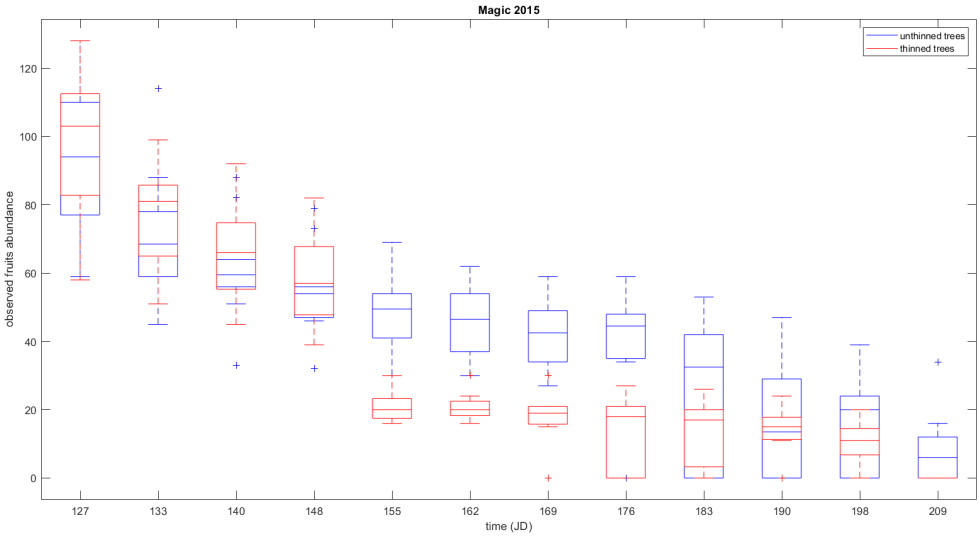

Figure 2.8: Fruit abundance over time, cv. Magic, 2015.

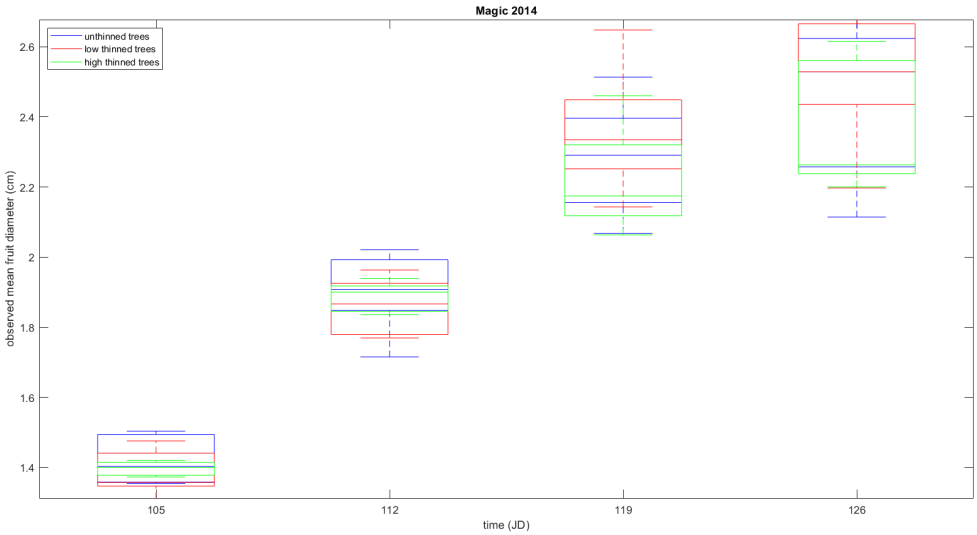

Figure 2.9: Average diameter d of a single fruit over time, cv. Magic, 2014.

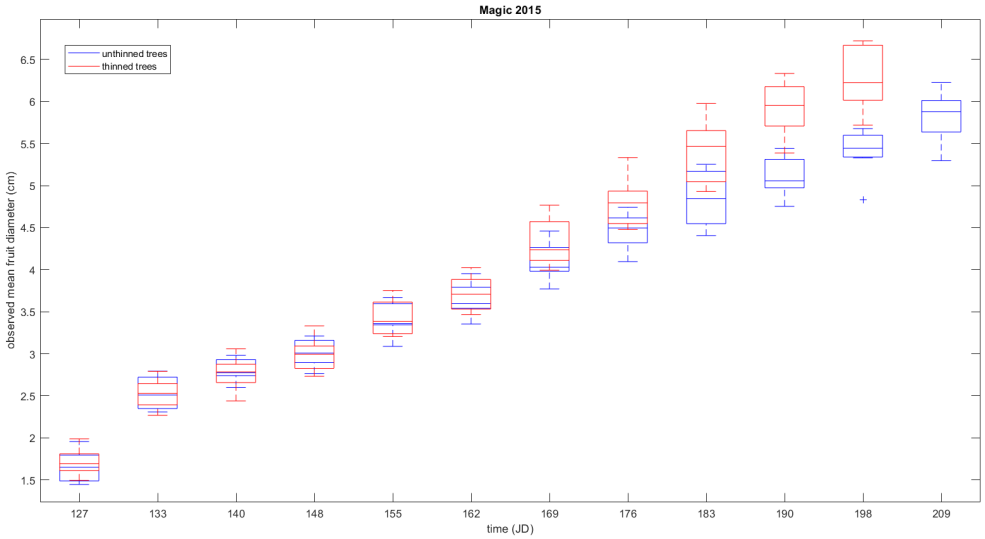

Figure 2.10: Average diameter d of a single fruit over time, cv. Magic, 2015.

2.1 Morphometric relations for fruits

Besides the data already presented, a smaller sample of both Magic and Suncrest fruits was collected in 2014 to investigate morphometric relationships. For each fruit, diameter was measured along with fresh weight FW (total weight of the organ) and dry weight DW (weight of the organ in a completely dry condition).

We first assumed that both relationships between fruit size and weight (fresh and dry) could be expressed by a two-parameter power law like the following one

$$y = \alpha x^{\beta} \tag{2.1}$$

Then we evaluated if and which of their parameters share the same value between fresh or dry weight and between fruit varieties. We took these two factors to perform an Analysis of Covariance (ANCOVA) on the linearized model derived from the previous one through logarithms

$$\log y = \log \alpha + \beta \log x \tag{2.2}$$

The analysis let us find the values of the slope β and of the intercept $\log \alpha$ of the regression while testing, at the same time, if their variations on any combination of cultivar and type of weight were statistically significant. It turned out that the allometric relationships share the same slope whether fruits are Suncrest or Magic, whether measured in terms of dry weight or fresh weight; indeed β was not significantly influenced by cultivar (p-value=0.0957 assuming a significance threshold of 0.05) and not influenced at all neither by type of weight (p-value=0.2608) nor by the combination of the two factors (p-value=0.5586). The resulting models (overall R^2 equal to 0.9834) can be seen in Figure 2.11 as they differ by their intercept values only.

In Table 2.3 the final calibrated parameters of the power law equation.

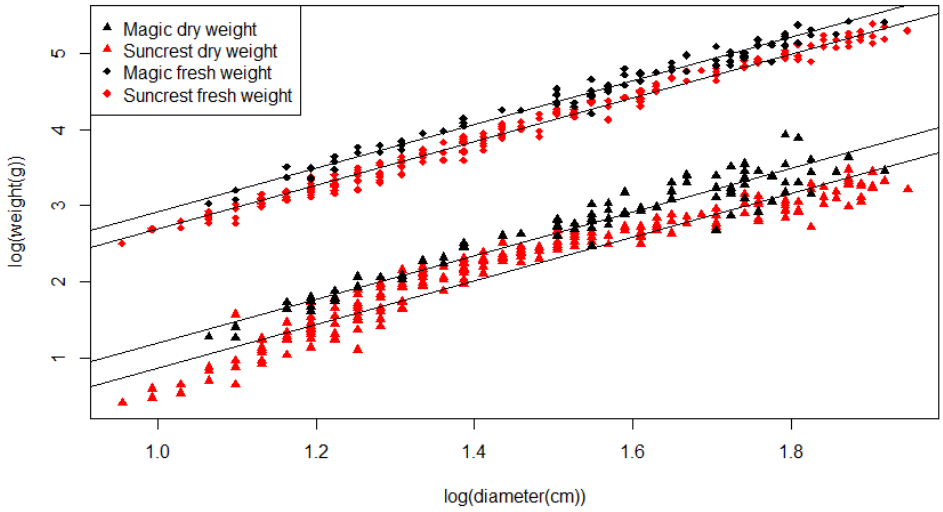

Figure 2.11: Fruit weight over diameter, in a logarithmic scale. Black lines are the fitting regressions, differing to each other only by the intercept value.

	α_{FW}	α_{DW}	β
Suncrest	0.8265	0.1336	2.87647
Magic	1.0388	0.1859	2.87647

Table 2.3: Parameter values of the power law equation, after the ANCOVA regression.

2.2 Morphometric relationships for shoots

As we did before with the fruits, we wanted to find a morphometric relashionship between the observed length of new shoots L and their dry weight DW. We did not have any coupled measurements of the two variables to compute a direct regression, but we did have two other datasets, one regarding shoot length together with their fresh weight and one regarding fresh and dry weight of shoots.

We used the first dataset to estimate the parameters of the allometry between shoot length and fresh weight, assuming it had the shape of a power law equation as the following

$$FW = \alpha L^{\beta} \tag{2.3}$$

and converting it into logarithm terms to compute a linear regression (adjusted R^2 equal to 0.9528), as can be seen in Figure 2.12.

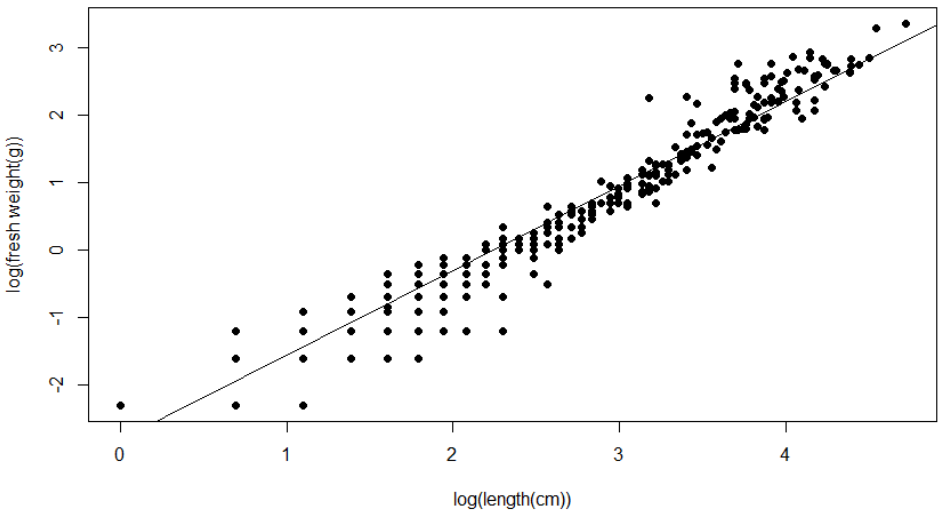

Figure 2.12: Shoot fresh weight over length, in a logarithmic scale.

Separately we estimated (adjusted R^2 equal to 0.9979, see Figure 2.13) the parameter describing the relationship between fresh and dry weight of shoots, assuming it had a linear shape with a null value of the intercept (trivial situation: if a shoot has no fresh weight, it has no dry weight either)

$$DW = \delta FW \tag{2.4}$$

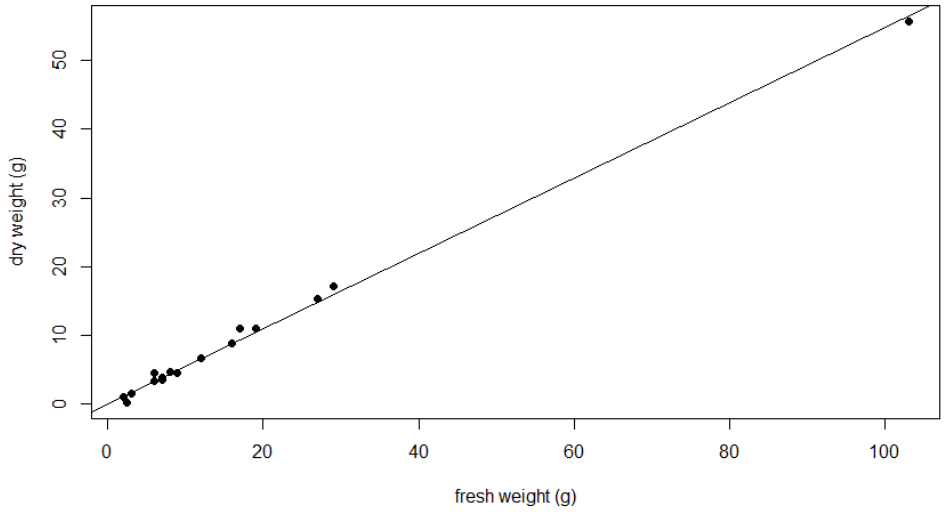

Figure 2.13: Shoot dry weight over fresh weight.

α	0.05990
β	1.25445
δ	0.54912

Table 2.4: Estimated values of the parameters.

The final calibrated parameters of the two relationships are listed in Table 2.4. From those, we could eventually assess a direct relationship between shoot length and dry weight, simply substituting equation 2.3 into equation 2.4 and coming up with the following

$$DW = \alpha\delta L^{\beta} = 0.03289 L^{1.25445} \tag{2.5}$$

Chapter 3

A mechanistic model for fruit tree growth

3.1 The original model

Thornley's model (1998), as it has been introduced in Chapter 1, rests on the conceptual framework presented in Figure 3.1. Overall, there is a total of six state variables, two of which representing the physical structure of the plant (total shoot biomass S and total root biomass R) and the other four representing its non-structural components, i.e. the nutrients available and distributed within the plant itself (carbon and nitrogen in the shoots, C_S and N_S, carbon and nitrogen in the roots, C_R and N_R).

The plant functioning is thus schematized through the interaction between an aerial section and an underground section, symmetrical to each other: inorganic carbon is assimilated from the atmosphere via photosynthesis through leaves and stored, mainly in leafy shoots; a fraction of this non-structural carbon is then transported downward to the roots. Similarly, inorganic nitrogen is assimilated by the roots through absorption and there it is stored; a fraction of this non-structural nitrogen is then transported

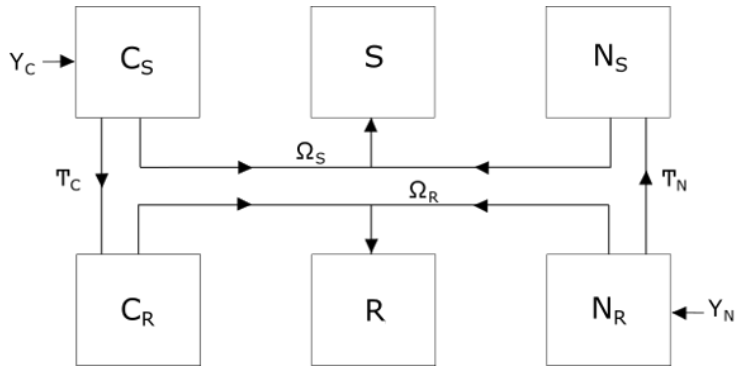

Figure 3.1: Conceptual framework of the original model.

upward to the shoots. These nutrients are eventually used to fuel plant's growth, being coupled and fixed in new structural matter.

The above-described processes can be translated into a six differential equations system describing each state variable changing over time.

$$\begin{cases} dC_S/dt = Y_C - \phi_C \Omega_S - T_C \\ dS/dt = \Omega_S \\ dN_s/dt = T_N - \phi_N \Omega_S \\ dC_R/dt = T_C - \phi_C \Omega_R \\ dR/dt = \Omega_R \\ dN_R/dt = Y_N - \phi_N \Omega_R - T_N \end{cases} \tag{3.1}$$

Where Y_C is the flux of carbon assimilated through photosynthesis (gC day^{-1}); Ω_S (grams of dry weight per day gDW day^{-1}) is the flux of non-structural dry matter transformed into new total shoot biomass S, expressed here in grams of dry weight; ϕ_C is the fraction of carbon; T_C is the flux of non-structural carbon transported from shoots to roots, while T_N is the flux of non-structural nitrogen transported from roots to shoots (gC day^{-1} or gN

day^{-1} respectively); ϕ_N is the fraction of nitrogen; Ω_R (grams of dry weight per day gDW day^{-1}) is the flux of non-structural dry matter transformed into new total root biomass R, expressed here in grams of dry weight; Y_N is the flux of nitrogen absorbed by roots as grams of nitrogen per day (gN day^{-1}).

Note that

$$\sum_j \phi_j < 1 \qquad j = C, N; \tag{3.2}$$

This is because plant organ matter is not made only by non-structural carbon and nitrogen, but also by other substrates (e.g. water or phosphorus) not explicitly represented in the model.

3.1.1 Carbon and nitrogen assimilation

Carbon assimilation is a function of photosynthetic activity, proportional to the leaf area which ultimately depends on the total shoot biomass; it is controlled by the concentration of non-structural carbon in leaves and by self-shading (Thornley 1998). We thus express it as

$$Y_C = \frac{\sigma_C S}{(1 + \frac{\Gamma_{CS}}{\iota_C})(1 + \frac{S}{K_S})} \tag{3.3}$$

where σ_c is the net rate of photosynthesis per unit of total shoot biomass (equal to 0.1 gDW^{-1} day^{-1}); the process decreases with the increase of S and with the increase of non structural carbon concentration in it, here defined as Γ_{cs}; it reaches its half when the total shoot biomass is equal to K_s=1000 gDW, the self-shading parameter, or when Γ_{CS} is equal to ι_C (0.1 gC gDW^{-1}), the inhibition rate parameter. We then express N assimilation by roots as

$$Y_N = \frac{\sigma_N R}{(1 + \frac{\Gamma_{NR}}{\iota_N})(1 + \frac{R}{K_R})} \tag{3.4}$$

where σ_N is the net rate of N absorption per unit of total root biomass (equal to 0.02 gN gDW^{-1} day^{-1}); similarly as before, ι_N (0.01 gN gDW^{-1}) is the inhibition rate parameter related to the nitrogen concentration in roots (Γ_{NR}) and K_R=1000 gDW is the competition parameter related to R.

3.1.2 Carbon and nitrogen allocation

Formation of new organic structure depends on a combination of substances of which carbon and nitrogen are the main components, both in a fixed ratio, and thus becoming the non-structural substrate to be allocated towards plant's tissues: growth stops if either one of the two substances is unavailable (Thornley 1972). We assumed the non-structural fluxes of dry matter to be proportional to the mass of the organ they are allocated towards, to the product of substrates concentration (reported here as Γ_{CS} and Γ_{NS} for the carbon or the nitrogen concentration in the shoots, Γ_{CR} and Γ_{NR} for the carbon or the nitrogen concentration in the roots), and to the plant efficiency in converting non-structural substrates into organic structure, expressed here by the parameter k having a constant value of 200 [gC gN gDW^{-2}]$^{-1}$ day^{-1}.

$$\Omega_S = k\Gamma_{CS}\Gamma_{NS}S \tag{3.5}$$

$$\Omega_R = k\Gamma_{CR}\Gamma_{NR}R \tag{3.6}$$

where eq. 3.5 refers to the substrates allocation to the shoots; similarly, eq. 3.6 refers to the substrates allocation to the roots.

According to Thornley, the value of the efficency parameter k is obtained assuming concentrations of substrates C and N equal to, respectively, 0.05

and 0.01 g (g of structural dry weight)$^{-1}$ considering a total growth rate of 0.1 day^{-1} overall.

3.1.3 Carbon and nitrogen transport

Non-structural C and N are transported from shoots to roots, and viceversa, thanks to a widespread system of capillaries formed by the so-called xylem and phloem (see Chapter 1). The process of the transport of carbon or nitrogen is described here as a substrate concentration difference, divided by a resistance (Thornley 1998).

$$T_C = \frac{(\Gamma_{CS} - \Gamma_{CR})}{(\frac{1}{S})^q + (\frac{1}{R})^q} \tag{3.7}$$

$$T_N = \frac{(\Gamma_{NR} - \Gamma_{NS})}{(\frac{1}{S})^q + (\frac{1}{R})^q} \tag{3.8}$$

where q introduces a scale factor to the resistance, which Thornley (1998) related to the plant architecture and set equal to 1.

3.2 From a generic plant to a deciduous fruit tree

The model we just described derives directly from Thornley's work (1998) and it translates into mathematical terms how a generic plant grows. In order to effectively simulate the growth of a more specific plant, a deciduous fruit tree, however, some processes must be taken into account and must be added to this basic structure: the seasonal changes on the tree vegetative growth and, of course, fruit abundance and development.

3.2.1 Seasonal vegetative growth

With the autumn and the winter approaching, the tree must prepare itself to the cold months ahead. It stops its vegetative growth (shoots and roots)

at the end of the growing season in late July in order to be able to spend the whole August and September gathering resources and storing them as reserves.

We described this process by modifying the fixed allocation parameter we started from in the original model, making it a sigmoid function over time.

$$k(t) = \frac{k_{max}}{1 + e^{-\eta_k(t-\lambda_k)}} \tag{3.9}$$

Where k_{max} has the same value of the previous constant parameter found by Thornley, while η_k is the slope of the sigmoid located at its half-saturation point λ_k.

From observations of shoot growth we could set λ_k equal to 198 JD (July 17th) and then we calibrated η_k considering we wanted the allocation to slow down from 90 percent to 10 percent of its former maximum in two weeks.

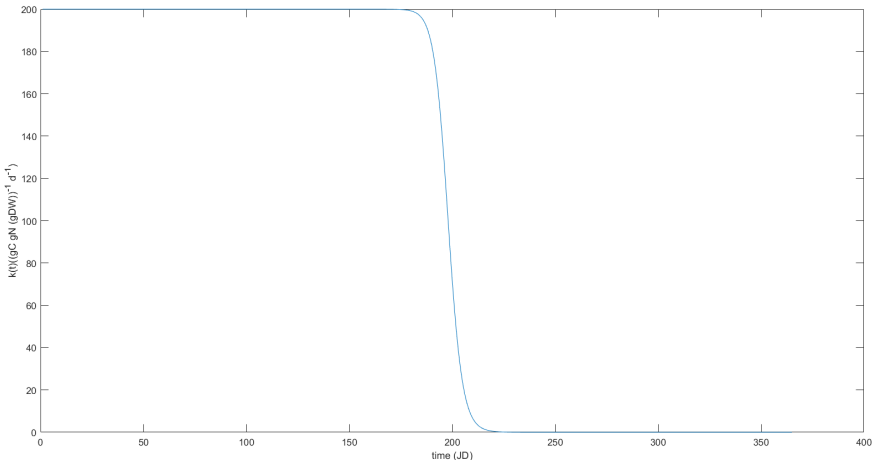

Figure 3.2: Substrates allocation function k(t)

3.2.2 Fruit growth

A fruit is a reproductive-specialized organ, developing from flower's ovary, which provides a suitable environment for seed maturation and often also a

mechanism for the dispersal of mature seeds (Gillaspy et al. 1993).
A variety of different classifications and descriptions of fruit growth pattern can be found in the literature, depending on which specific aspect of growth we are interested in and depending on the specific type of fruits. In a majority of species, the increasing volume or mass over time has a sigmoid shape and the recognition of three main stages is generally accepted: starting right after anthesis, which is the flower life-time, a first rapid phase of cell division is followed by an exponential growth phase of cell enlargement, as they behave as sinks of plant resources; eventually it leads to a final phase of maturation and slow growth referred as ripening.

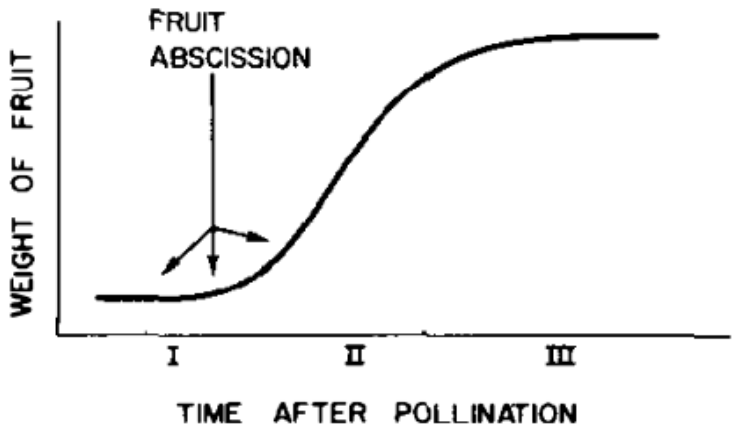

Figure 3.3: Single sigmoid growth (Stephenson 1981)

In the case of stone fruits, among which peaches are included, instead, the second stage is preceded by another exponential expansion and then by another slow growth phase, due to seeds enlargement and pit hardening respectively, overall forming a double sigmoid growth curve (Stephenson 1981, B.G. Coombe 1976).

Despite the lack of data and of proper studies in the literature, it is reasonable to assume that most of the initial exponential fruit growth is sustained by reserves stored by the tree during the previous growth season.

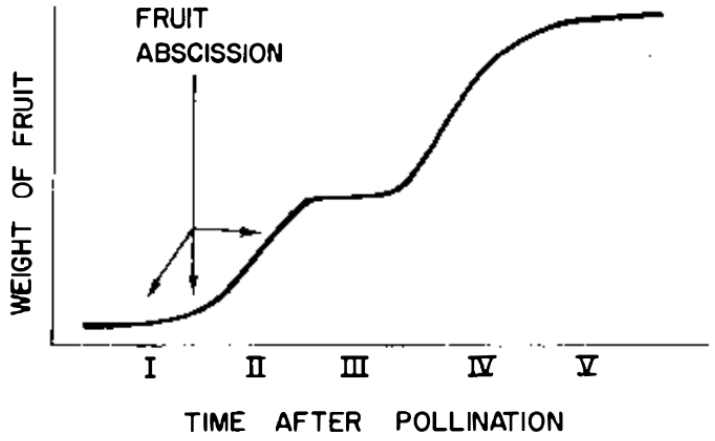

Figure 3.4: Double sigmoid growth (Stephenson 1981)

That's because, for a few weeks after bud break, the shoots leaf area could not be sufficient to provide photosynthates out of those needed to its own increase: thus, the plant could be forced to mobilize and to use its nutrient reserves, stored during the previous years, until shoots are developed enough.

3.2.3 Fruit abundance

The maximum number of fruits produced by a tree is set at the start of the growing season and derived from buds abundance, inflorescence and pollination; then, trees can only drop and lose fruits through the closure of the Abscission Zone (AZ), a region of functionally specialized cells usually sited in the boundary between the organ and the body plant, triggered by developmental or environmental or even hormonal cues (Estornell et al. 2013).

The number of fruits is subjected to two rapid decreases concentrated in very recognizable periods: one fruit abscission early in the growth season, regulating and limiting the initial fruit set in order to reduce competition of assimilates between fruits themselves; the abscission precedes the (first)

exponential growth phase of the organ so that the plant does not invest too many resources in fruits that will not perform their reproductive role because aborted (Stephenson 1981; see Figure 3.3 and Figure 3.4); a second loss occurs during the final growth stage instead, while the fruits are close to their maximum size and therefore they are ripening and slowly senescing. We will refer to these phases as Early Abscission and Ripening Loss.

3.3 The modified model

Considering the processes we just described, we can now present a new conceptual framework for our model as can be seen in Figure 3.5.

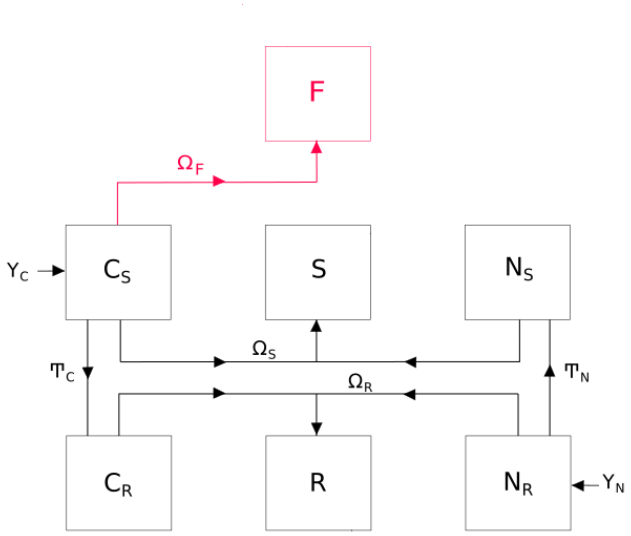

Figure 3.5: Conceptual framework of the modified model. Note that F is the total fruit biomass.

A new flux of nutrients Ω_f draws from the non-structural carbon in shoots and it is redirected towards the fruits to be converted into new structural matter, making the reproductive growth compete with the vegetative growth of shoots and roots. Therefore we had to take into account two new variables, total fruit biomass being described by the average fruit biomass

f and the fruit abundance n_f. Note also that we divided the total shoot biomass S too, separating the average shoot biomass sh from the total number of shoots n_{sh} (which we assumed to be constant).

$$\begin{cases} dC_S/dt = Y_C - \phi_C \Omega_S - T_C - \phi_{Cf} \Omega_f \; n_f \\ dsh/dt = \frac{\Omega_S}{n_{sh}} \\ dn_{sh}/dt = 0 \\ dN_S/dt = T_N - \phi_N \Omega_S \\ dC_R/dt = T_C - \phi_C \Omega_R \\ dR/dt = \Omega_R \\ dN_R/dt = Y_N - \phi_N \Omega_R - T_N \\ df/dt = \Omega_f \\ dn_f/dt = -\mu \; n_f \end{cases} \tag{3.10}$$

The system of equations has been modified accordingly, where ϕ_{cf} is the fraction of Carbon composing the flux of resources being drawn by the fruits, while μ (day^{-1}) is the fruit drop rate.

3.3.1 Allocation to fruits

According to the existing literature about fruit modeling, and given the lack of data and basic knowledge regarding the amount of nitrogen in the fruit flesh, we assumed carbon is the only substance whose contribution to fruit growth is not negligible.
Therefore, we defined

$$\Omega_f = k_f \Gamma_{CS} (1 - f/\chi) f \tag{3.11}$$

where k_f is the plant efficiency in converting non-structural carbon into new fruit biomass ([gC gDW^{-1}]$^{-1}$ day^{-1}), the amount of nutrient available being regulated by a concentration gradient between the shoot and the fruit itself: however, we assumed that non-structural carbon within the fruit is converted immediately and so the gradient is always equal to Γ_{CS} itself; we then defined χ as equal to the maximum dry weight a single fruit can reach, depending on cell number and cell maximum expansion, and limiting its further development (Grossman and DeJong 1994).

Chapter 4

Model calibration

4.1 Offline calibration

According to Stephenson (1981), in the earliest stage of fruits growth the tree must allocate and divide its resources in order to generate and to develop fruits seeds in a certain number. Seeds, then, assume the role of sources of hormones which inhibit the activation of the Abscission Zone and attract even more assimilates from the tree: fruits subjected to Early Abscission are therefore those which have fewer seeds at anthesis, thus those which have smaller mass due to rather late development or competition with other fruits for nutrition. Mass can be related also to the second period of drop (Ripening Loss) if we consider gravity, i.e. if we assume to be reasonable to expect higher values of drop rate for bigger and heavier fruits approaching some mechanic limit of the bearing capacity of the stems.

Therefore, taking into account the average mass of a single fruit allows us to sum up the two different phenomena behind fruits drop with a single, intrinsic, explanatory variable. We defined and investigated two types of function formed by the interaction between both the mechanisms we just described.

$$\mu(t) = ax^{k_1} + bx^{k_2} \tag{4.1}$$

$$\mu(t) = ae^{k_1 x} + be^{k_2 x} \tag{4.2}$$

Where a and k_1 are parameters related to the Early Abscission while b and k_2 to the Ripening Loss. We expected the values of these parameters to make the two addends qualitatively symmetrical and opposite to each other, but we did not know which function was able to better describe the phenomenon; moreover, we could adopt either the fresh or the dry weight of the fruits as explanatory variable, and we wanted to check which one leads to the best fit of the data.

Excluding the observations affected by thinning, we derived the fruit drop rate $\mu(t)$ from the observed fruit abundance of both Magic and Suncrest measurements with the following equation

$$\mu(t) = -\ln\left(\frac{N_{f\ t+1}}{N_{f\ t}}\right)\frac{1}{\Delta t} \tag{4.3}$$

and then we calibrated each function separately with both the dry and the fresh weight samples derived from our fruit diameter dataset thanks to the morphometric relationships we defined in Chapter 2. Calibration was performed finding the two sets of parameters, a different one for each cultivar, that minimized the Residual Sum Squared

$$RSS = \sum_{j} \sum_{i=1}^{n} (\mu_i - \hat{\mu}_i)^2 \tag{4.4}$$

where n is the number of samples from the cultivar j (Suncrest or Magic), μ_i is the i-th drop rate observation and $\hat{\mu}_i$ its estimated value. The best function and the best type of weight combination to adopt is therefore the one having the lowest value of RSS: we can check the results in Table 4.1.

Type of weight	Type of function	RSS
DW	(4.1)	0.111775
	(4.2)	0.122853
FW	(4.1)	0.110301
	(4.2)	0.119303

Table 4.1: Residuals Sum Squared comparison between different combinations of function and type of weight.

According to the RSS, the calibrated parameters of the power law equation (4.1) best minimize the distance between observations and estimated values of fruit drop rate if we use the fresh weight as explanatory variable.

Before fixing these parameters though, a second step was made aiming to investigate if we could have a more parsimonious model, with some of the parameters sharing common values. Indeed we could identify similar physical meaning to couple of parameters that therefore could potentially have the same value without reducing the quality of the fit: both a and b are referable to respectively the Early Abscission drop rate and the Ripening Loss drop rate of a single unit of weight; both k_1 and k_2 are referable to the intensity of respectively the Early Abscission hormonal activity and of the gravity on the mechanical resistance of the petiole of the fruits during the Ripening Loss.

In order to do so, we used the corrected Akaike Information Criterion AIC_c which quantifies the best compromise between goodness of fit and parsimony. It is defined as

$$AIC_c = AIC + \frac{2k(k+1)}{n-k-1} \qquad AIC = 2n\left[ln\left(\sqrt{\frac{RSS}{n}}\right) + \frac{k}{n}\right] \tag{4.5}$$

where k represents the number of parameters characterizing the model, n represents the number of observations and RSS the Residuals Sum Squared as it has been already presented before. Thus, a more complex model is

preferred to a simpler one only when the logarithm of Residuals Root Mean Square $ln\left(\sqrt{\frac{RSS}{n}}\right)$ decreases more than the increase of the ratio between the number of parameters and the number of data ($\frac{k}{n}$).
The lowest AIC_c value of model M1 (i.e. equation (4.1) selected earlier) shown in Table 4.2 proved that is better to keep all the parameters separated during the calibration (note that the total number of parameters k counts the two sets needed for both Suncrest and Magic cultivar).

Model	**Restriction**	**k**	**RSS**	$\boldsymbol{AIC_c}$
M1	none	8	0.110301	-5658.6203
M2	$k_1 = k_2$	6	0.138139	-5572.7558
M3	$a = b$	6	0.143482	-5557.5762
M4	$a = b$ and $k_1 = k_2$	4	0.144367	-5559.2290

Table 4.2: List of the Akaike Index value for every case considered. Note that the model M1 is the equivalent of equation (4.1) from the previous selection.

A final step was made trying to find any possible similarity between different peach cultivars. It seems reasonable to expect that, having the same mechanisms behind fruit drop, they may share the same value for at least some of their parameters too: we applied the M1 model again to both our Suncrest and Magic sets of data, this time trying several combinations of common parameters to calibrate. Every case we thus defined is listed in Table 4.3, coupled with its own value of AIC_c to be compared for the selection.

Model	Common Parameters	k	RSS	AIC_c	ΔAIC_c
M11	k_1 and k_2	6	0.110339	-5662.6370	-
M6	k_2	7	0.110123	-5661.3489	1.2881
M8	b	7	0.110253	-5660.8769	1.7601
M5	k_1	7	0.110336	-5660.5759	2.0611
M14	k_2 and a	6	0.111017	-5660.1867	2.4503
M12	a and b	6	0.111273	-5659.2654	3.3716
M7	a	7	0.110755	-5659.0598	3.5772
M1	none	8	0.110301	-5658.6203	4.0167
M13	k_1 and b	6	0.111975	-5656.7498	5.8872
M17	k_1, a and b	5	0.114320	-5650.5208	12.1162
M15	k_1, k_2 and a	5	0.114394	-5650.2620	12.375
M9	k_1 and a	6	0.114289	-5648.5679	14.0691
M16	k_1, k_2 and b	5	0.121790	-5625.2022	37.4348
M10	k_2 and b	6	0.121206	-5625.0633	37.5737
M19	all	4	0.123787	-5620.7475	41.8895
M18	k_2, a and b	5	0.123471	-5619.7189	42.9181

Table 4.3: Output of the Akaike selection, testing common parameters between different cultivars.

Models having an index value within 2 points to each other are considered equal (Symonds and Moussalli 2011, Burnham et al. 2011) and are highlighted in the table. We had no other best-fitting based criteria to select a model between those first three, so we chose M11 aiming to keep it as simple as possible with the lowest amount of parameters: by implication, doing so we tested that the action of the hormones on the Abscission Zone and the action of the gravity on the petiole of the fruit do not depend on cultivar, instead their intensities are equal regardless of which variety we are considering.

Finally, we can adopt and fix the values of the parameters obtained in the last calibration accordingly to model M11 (see Table 4.4 and Figure 4.1).

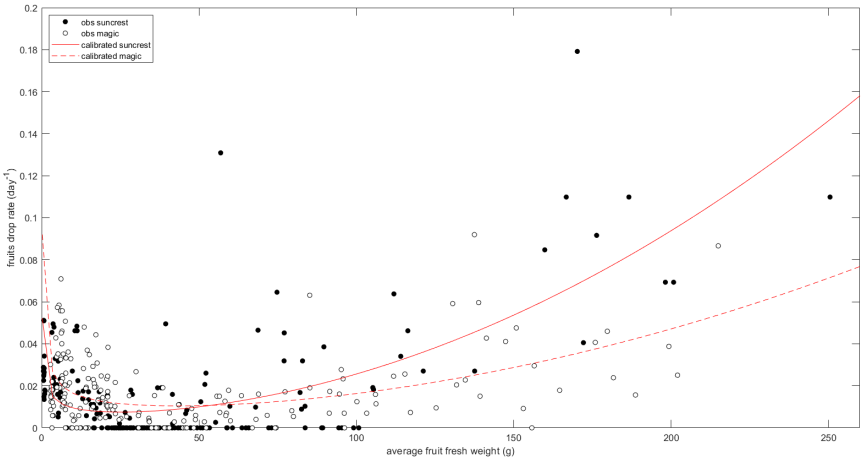

Figure 4.1: Fitting curves of the observed drop rate, according to model M11.

Type of Cultivar	**Model**	**a**	**b**	k_1	k_2
Suncrest	$aFW^{k_1} + bFW^{k_2}$	0.0256	$1.887 * 10^{-6}$	-0.4415	2.0360
Magic		0.0452	$8.827 * 10^{-7}$	-0.4415	2.0360

Table 4.4: Final value of the calibrated parameters, having adopted a power law model with Fresh Weight (FW) as explanatory variable.

4.2 Online initialization and calibration

Since we had most of the values of the parameters of the model either already found by Thornley himself or calibrated manually by us (see the vegetative growth efficiency $k(t)$ in Chapter 3) or calibrated offline as it was the case for the fruits drop rate, we needed to calibrate only a few parameters left before running the entire model.

The first one is the plant efficiency in converting non-structural carbon into new fruit biomass k_f. We assumed this parameter to be constant over time while competing in resources with the vegetative growth; when the develop-

ment of shoot biomass starts to switch off with the approach of the autumn, k_f does not decrease instead and the nutrients available are directed towards the fruits only, making their second growth phase possible.
The second parameter we calibrated was σ_c, the net rate of photosynthesis per unit of shoot biomass. Despite its value was already given by the original model (Thornley 1998), it considers implicitly both the net rate of photosynthesis per unit of leaf area and the morphometric relationship between shoot biomass and leaf area: it seems reasonable to expect, therefore, that at least this last relation can change slightly between different plant species, and so can the value of σ_c overall.

We performed the calibration by finding the set of parameters that minimizes the average Fraction of Variance Unexplained, defined as

$$FVU = \sum_i \sum_k \frac{\sum_t (y_{i,k,t} - \hat{y}_{i,k,t})^2}{\sum_t (y_{i,k,t} - \bar{y}_i)^2} \tag{4.6}$$

where $y_{i,k,t}$ is the observed value of variable $i = N_f$, N_{sh}, d, l_{sh} of tree k collected at time t, $\hat{y}_{i,k,t}$ is its corresponding estimated value (in case of fruit diameter d and shoot length l_{sh} they are converted back from sh and f value thanks to the morphometric relationships of Chapter 2) obtained from the model and depending on the set of parameters, and $\bar{y}_i$ is the average value of the observations over all the trees and the sampling times (Bruchou and Génard 1999).
The main advantage of using this type of cost function is that errors are normalized with respect to the variance of each variable considered, regardless of their unit of measurement or variation range, therefore they can be compared and summed at once.

The initial values of the variables of the model were taken from observations when possible, thus in case of fruit abundance, fruit average diameter,

shoot abundance and average length; we set the initial value of root biomass R_0 being proportional to the one-year-old shoots grown during 2012 before being pruned at the beginning of 2013, knowing how to convert shoots length into dry mass thanks to the relations found in Chapter 2 and knowing the optimal equilibrium between shoots and roots Dry Mass equal to 0.22 (Grossman and DeJong 1994); finally, we set the values of the non-structural variables as fractions of their respective structural compartments following the example of Thornley 1998): C_S and C_R are 5% of the initial values of shoot and root biomass respectively, while N_S and N_R are 1% of the initial values of shoot and root biomass respectively.

The final values of the parameters are $k_f = 18.1412\ [gCgDW^{-1}]^{-1}day^{-1}$ and $\sigma_c = 0.2362\ gDW^{-1}day^{-1}$, given a FVU equal to 11.1378.
The results of the calibration are presented in Figure 4.2, where observed and simulated values of each variable are plotted and compared: ideally a perfect model would show all the points along the bisector, meaning having no discrepancy between the simulation and the reality; instead, the distance of the points from the bisector represents either the overestimation or the underestimation of the observations by the model.
While taking into account the variable n_{sh} was trivial due to the assumption of constant abundance of shoots, it is noticeable the general good fitting of the model especially in the case of fruit abundance n_f and shoot average length l_{sh}.

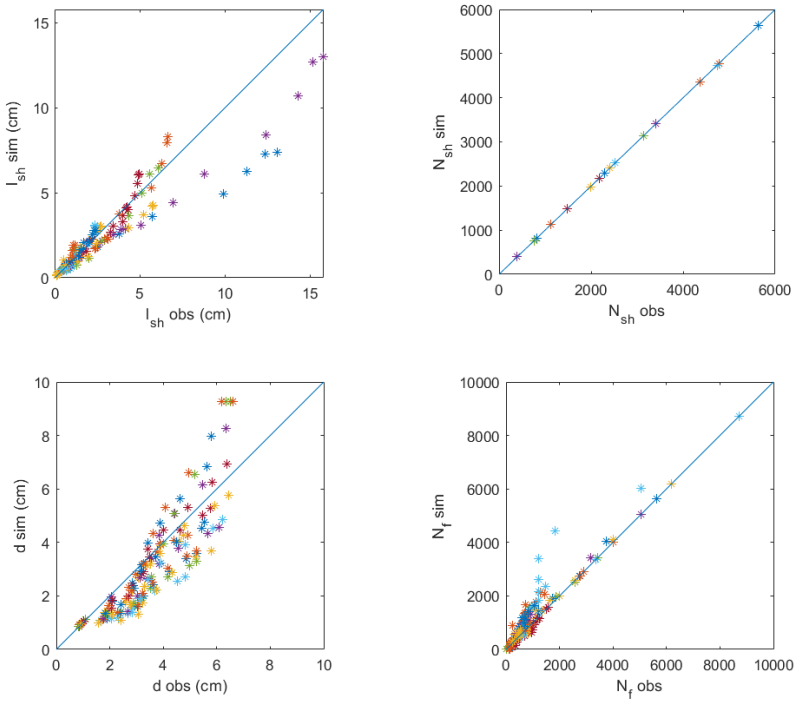

Figure 4.2: Comparison between observed and simulated values of the model, after the calibration. Points with same color belong to the same tree.

The average diameter of the fruits d, despite being good at the end of the fruit growth when fruits are at their maximum dimension, is underestimated systematically during the first phases of development, while fruits have within 2 and 4 centimeters of diameter.

This is presumably because we are not considering the role of the reserves of the tree, gathered the year before, acting as the main source of supply and fuel for the fruits during their first weeks after bloom. Up to that point, shoots have indeed no sufficient leaf area to provide enough photosynthate for both vegetative and reproductive development and the plant must rely on stored nutrients until it becomes a net assimilator (Andersen and C. Schaffer 1994).

Chapter 5

The multiannual model

Several studies and modeling attempts have been made recently in order to understand and describe the main factors regulating the transition of deciduous trees over years. Most of them are focused on the masting phenomenon, well known in forest ecology (Hartmann and Trumbore 2016), meaning the episodic synchronous production of large seed crops by plant populations at the landscape level.

Only a few exceptions in the literature show interest in resource budget models for individual plants (Isagi et al. 1997), but in these cases plant physiology during the growth season is only marginally considered if not neglected at all. Once established a solid mechanistic model describing the plant's growth over a single season, we tried to expand it and make it able to cover the simulation of sequential years of alternating growth and dormancy periods to overcome the limits of both the different approaches cited above. We coupled our continuous-time system of equations (3.10 in Chapter 3) with a set of discrete-time relations which summarizes and schematizes all the physiological processes happening from the late autumn, when the tree enters in the phase of resting and minimizes metabolic activity, to the early spring.

Tree id	$S_{left2013}$	$S_{left2014}$
1	20.82	20.95
2	86.83	42.78
3	43.72	28.71
5	11.49	30.62
6	84	59.54
7	161.98	35.07
8	29.93	17.89
9	66.27	55.11
10	151.83	53.14
11	156.13	129.43
12	91.74	56.46
13	16.9	15.36
15	73.54	77.63
17	51.45	68.49
18	126.7	91.84
19	27.9	29.48
20	59.86	111.97

Table 5.1: Observed total one-year-old shoot length left after pruning at the beginning of 2013 and 2014.

5.1 Fruit and shoot abundance

We made the simple assumption that the number of fruits and the number of new shoots are proportional to the total length of one-year-old shoots, meaning the total shoot biomass S that has grown during the previous year. Therefore, we consider the plant as having a constant "density" of buds set at the beginning of every growth season.

We gathered the data of the initial number of fruits and shoots in 2013 and 2014 and we coupled it with the total length of one-year-old shoots grown during 2012 and 2013, respectively, expressed in meters. The length values were taken after subtracting the total shoot length cut by pruning. In both years, pruning occurred at the end of January when the buds were not broken yet: for this reason, we named the variable total one-year-old shoot length left S_{left}, whose values are presented in table 5.1.

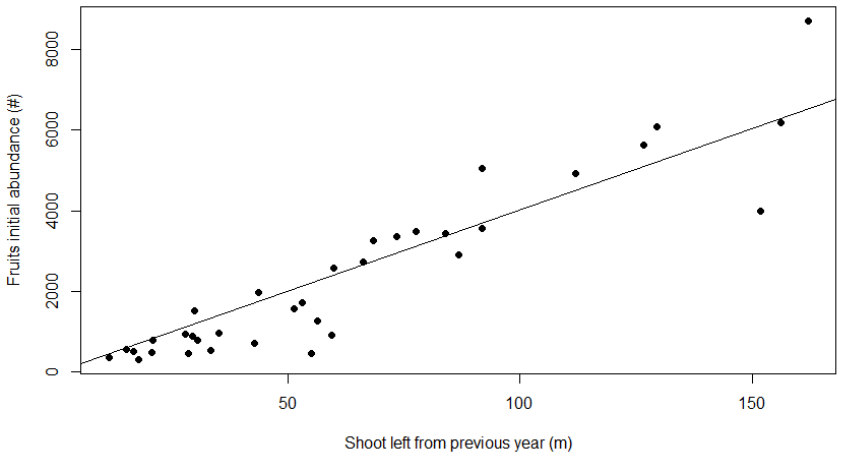

Figure 5.1: Linear regression of initial fruit abundance against total one-year-old shoot length left after pruning.

We performed linear regressions for both initial fruit abundance and initial shoot abundance against the total one-year-old shoot length left; we imposed the trivial condition of having no fruits nor shoots if there is no S_{left} at the beginning of the year, meaning both regression lines have an intercept value equal to zero.

The regression involving fruit abundance had an adjusted R squared equal to 0.9320 with a calibrated coefficient value of 40.206 (p-value $<$ 2.2e-16), while the regression involving shoot abundance had an adjusted R squared equal to 0.9292 with a calibrated coefficient value of 40.777 (p-value $<$ 2.2e-16), so that

$$n_{f0} = 40.206 \cdot S_{left} \tag{5.1}$$

$$n_{sh0} = 40.777 \cdot S_{left} \tag{5.2}$$

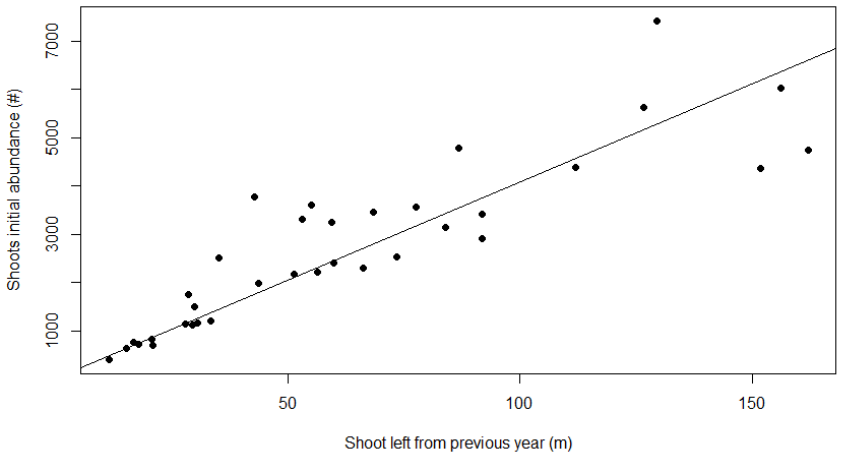

Figure 5.2: Linear regression of initial shoot abundance against total one-year-old shoot length left after pruning.

5.2 Average size of fruits and shoots

As we already mentioned at the end of Chapter 4, it is known that reserves play a major role in providing early nutrient supply for fruits and presumably also for shoots, especially at bud offset when the tree is not able to perform photosynthesis yet. However, the knowledge of storage dynamics, its control and responses to environmental stresses is very limited, even after a century of research (Hartmann and Trumbore 2016): this may be due to several reasons, like the difficulty in recognizing the various forms that reserves can assume (non-structural carbohydrates NSC, starch, proteins) and their usage over different temporal scales, or in observing how they are stored and allocated (Silva et al. 2013).

As we approached the modeling of how the size of new fruits and shoots is determined at the beginning of the season, we made the cautious assumption that in both cases it is influenced by the S_{left} already defined, considered as

a proxy variable of the reserves accumulated during the previous year. In fact, as we already mentioned in paragraph 4.2, shoot development competes for resources with fruits, whose growth is the main store depletion sink: the more the shoots have grown, the less total fruit biomass has been produced, and therefore the more reserves have been accumulated.
Then, given the lack of theoretical information in the literature, we assumed that the size of new fruits and shoots is influenced also by the meteorological conditions occurred between the blooming and the first observation, as we did not monitor photosyntethic capacity of the plants (i.e. the already growing shoots) during those windows of time each year.
We expressed our hypotheses in the shape of an exponential equation like the following one:

$$y_0 = a \cdot \exp\left(-\frac{b}{CDD} - \frac{c}{S_{left}}\right) \tag{5.3}$$

where y_0 is either the fruit average diameter d_0 or the shoot average length l_{sh0}. CDD refers to the Cumulative Degree Days, which is an index synthesizing the cumulative temperatures occurring during a period of time; it is computed first by setting a degree threshold above which the developmental activities of the plant are influenced by temperature; then, the difference between the daily mean temperature and the threshold is calculated for each day of the time window of interest; finally, positive differences are summed up.

We considered a degree threshold of 7°C (Grossman and DeJong 1994) and the days between the bud burst and the first observation collected as time window.
Daily temperatures were measured at the INRA meteorological station close to the orchard, leading to CDD values equal to 272.7 for 2013 and to 315.15 for 2014: note that if in 2013 the blooming date was 1^{st} March and the first

observation was made at 30^{th} April, meaning a time window of 61 days, in 2014 instead it was only 47-day-long (blooming date at 9^{th} March and first observation at 24^{th} April) but its CDD value was much higher nonetheless. We thus expected bigger fruit diameters and longer shoots in 2014.

After having linearized the exponential equation via logarithmic transformation, we performed a linear regression with the 2013 and 2014 data in order to calibrate the six parameters a, b, c for fruits and shoots.
While both CDD and S_{left} had a significant effect on shoot average length, with a p-value $<<$ 0.001, fruit average diameter was not affected by S_{left}, which had an associated p-value of 0.946. Below we report the value of all the parameters of the relations converted back to the exponential form, coupled with their adjusted R squared (R^2_{adj}), and we plot the final curves superimposed to the data in Figure 5.3 and 5.4.

$$d_0 = 90.3779 \cdot \exp\left(-\frac{1248}{CDD}\right) \qquad R^2_{\text{adj}} = 0.9217 \tag{5.4}$$

$$l_{sh0} = 3.3264e+07 \cdot \exp\left(-\frac{5025.730}{CDD} + \frac{21.710}{S_{left}}\right) \qquad R^2_{\text{adj}} = 0.8842 \tag{5.5}$$

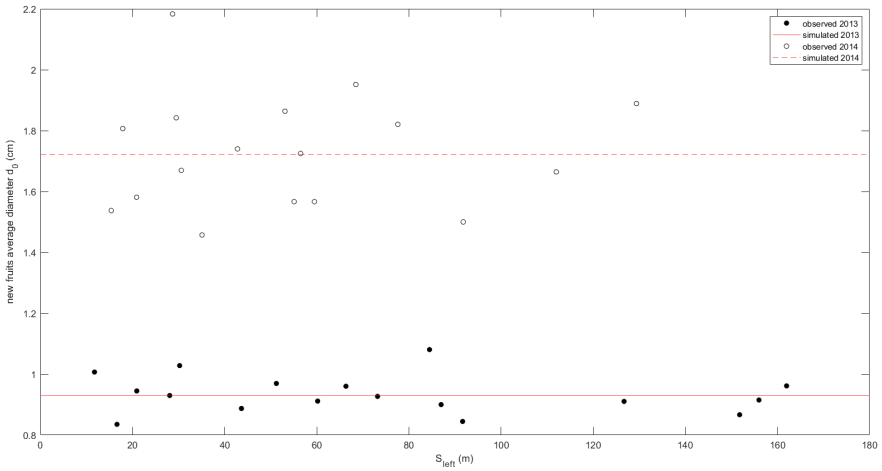

Figure 5.3: Calibrated curves of the relationship between total one-year-old shoot length left and initial fruit average diameter.

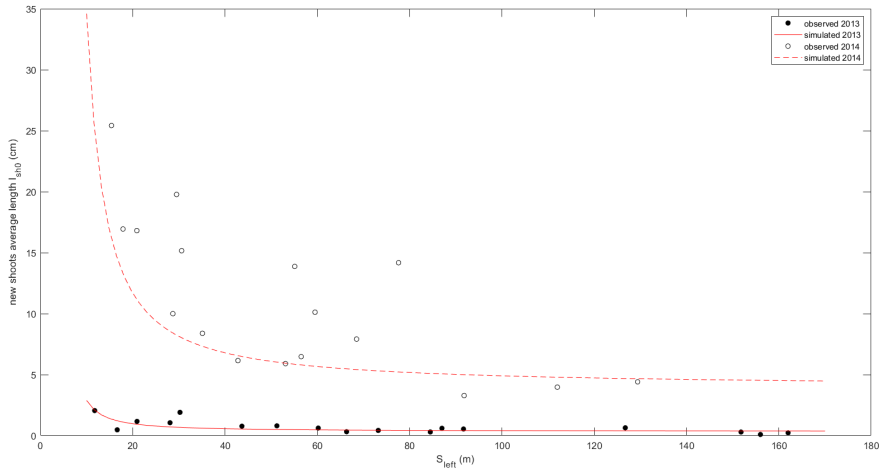

Figure 5.4: Calibrated curves of the relationship between total one-year-old shoot length left and average initial shoot average length.

5.3 Annual initialization

The relationships we found above provide, at the beginning of each growth season, the initial condition of fruit and shoot abundance n_{f0} and n_{sh0}, the average initial fruit diameter d_0, the average initial shoot length l_{sh0}.
Now we are able to estimate everything we need to initialize the continuous-time model at each iteration: thanks to the morphometric relationships we defined in Chapter 2, we can calculate the average initial fruit biomass f_0 from fruit diameter values and the average initial shoot biomass sh_0 from shoot length values; as we already initialized the model in Chapter 4, we can obtain the initial root biomass R_0 being proportional to the total one-year-old shoot length before pruning S_{np}, expressed here in centimeters, and we can obtain the initial value of the variables C_{S0}, C_{R0}, N_{S0}, N_{R0} as fractions of shoot or root biomass.
The following discrete-time model combines all the equations we explained above.

$$\begin{cases} C_{S0} = 0.05\ sh_0\ n_{sh0} \\ sh_0 = 0.03289\ [3.3264e+07 \cdot \exp\left(-\frac{5025.730}{CDD} + \frac{21.710}{S_{left}}\right)]^{1.25445} \\ n_{sh0} = 40.777\ S_{left} \\ N_{S0} = 0.01\ sh_0\ n_{sh0} \\ C_{R0} = 0.05\ R_0 \\ R_0 = 0.22\ [0.03289\ (S_{np})^{1.25445}] \\ N_{R0} = 0.01\ R_0 \\ f_0 = 0.1336\ (90.3779 \cdot \exp\left(-\frac{1248}{CDD}\right))^{2.87647} \\ n_{f0} = 40.206\ S_{left} \end{cases} \tag{5.6}$$

5.4 Model simulation

We used data from the beginning of 2013 and the beginning of 2014 to calibrate the discrete-time relationships which regulate the initialization of every year, keeping our 2014 and 2015 data to validate the final multiannual model.

The final values of l_{sh} from the simulation we showed in Chapter 4 were multiplied by the final values of shoot abundance n_{sh} to find the total one-year-old shoot length before pruning, S_{np}, and therefore to find R_0, the initial root biomass; S_{np} values were multiplied by the Pruning Intensity PI (listed in Table 5.2) each tree was subjected to at the beginning of 2014, so quantifying S_{left}.

From this point, thanks to the equation system (5.6), we were able to find all the initial conditions we needed: we computed a second iteration of the continuous-time model for 2014, eventually leading to new final values of the state variables. Once more, we were able to repeat the process of initializing the next year, knowing again the Pruning Intensity affecting the trees and the amount of CDD between the blooming date and the first observation (equal to 229.75); we had no records about the thinning date, so we simply assumed it was the same as in 2014.

Tree id	PI_{2014}	PI_{2015}
1	0.92	0.79
2	0.00	0.00
3	0.49	0.58
5	0.87	0.87
6	0.54	0.73
7	0.00	0.64
8	0.91	0.00
9	0.50	0.68
10	0.00	0.00
11	0.00	0.00
12	0.00	0.00
13	0.92	0.83
15	0.60	0.68
17	0.54	0.68
18	0.00	0.00
19	0.91	0.84
20	0.53	0.43

Table 5.2: Pruning Intensity adopted for each tree at the beginning of 2014 and 2015.

In Figure 5.5 we present the simulation computed over the year 2014; similarly as we did for 2013, we put the observed values of the variables along the x-axis and the simulated values along the y-axis, therefore better visualizing the quality of the model.

As it can be noticed, this first iteration shows a few weaknesses already: average shoot lengths are overestimated no matter which tree we are considering and especially for trees number 1 and 13 (the blue one and the green one in the plot, respectively), while fruit abundance becomes closer to the observations just at the end of the season (small values of n_f) having cases of both overestimation and underestimation otherwise. Simulated average fruit diameters are quite good though, despite a final spike which was not observed and presumably caused by an excess of photosynthesis of the overgrown shoots. Most of shoot abundances values are acceptable as well.

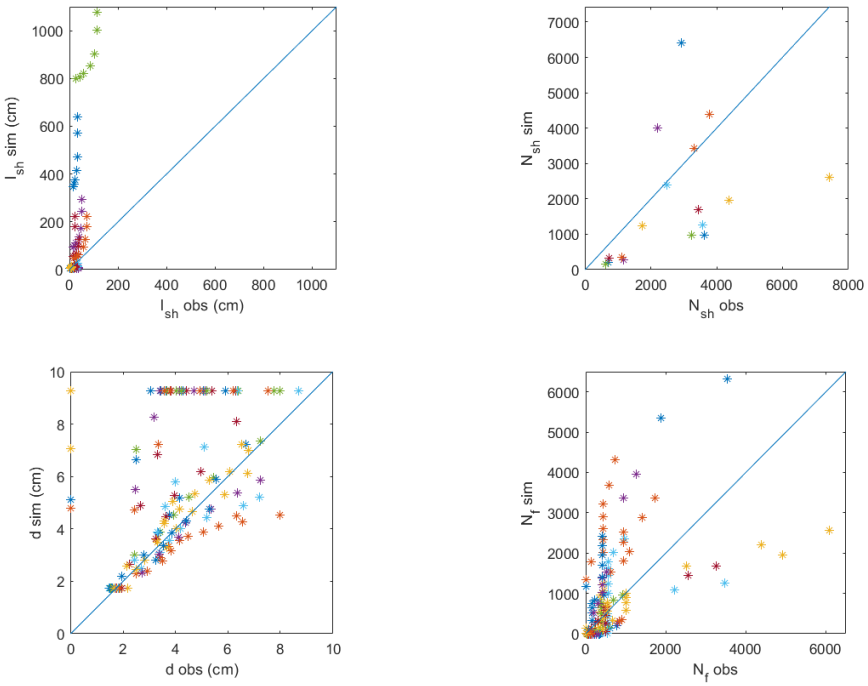

Figure 5.5: Comparison between observed and simulated variables of the model over the year 2014. Points with same color belong to the same tree.

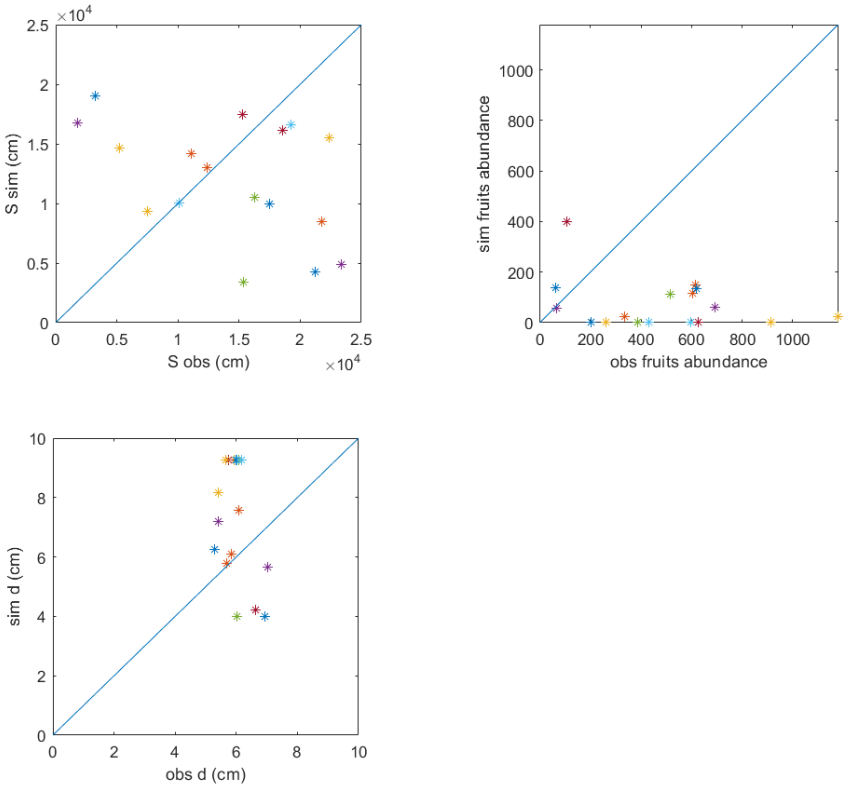

Figure 5.6: Comparison between observed and simulated variables of the model over the year 2015. Points with same color belong to the same tree.

Considering how we constructed the model, errors in the simulation of 2014 propagated to the initial conditions of 2015 and throughout its iteration. Having only the final values of the variables as they are reported in Chapter 2, we could not analyze the overall performance during the growth season as we did for 2013 and 2014, and we had to combine the average shoot length and the shoot abundance to be compared with our observed final total shoot biomass S.

That said, none of the simulation outputs seems to fit the collected data satisfactorily: fruit abundances tend to be underestimated, while both average fruit diameter and the total shoot biomass are noticeably spread at various distances from the bisector they should fit.

Chapter 6

Conclusions and discussion

Working at this thesis we achieved several results.

We presented an original model, based on that of Thornley (1998), which we took as a generic structure for a new model to be built on: we specified it for an individual deciduous fruit tree, adding the mathematical equations needed to describe the phenological rhythms proper of a tree and also the main physiological aspects of the dynamics of the fruits - their growth in term of biomass accumulation and their total abundance over the season. Fruits behave like sinks of nutrients constantly competing with the shoot development, and their initial number is regulated and gradually reduced by both hormonal and exogenous factors.

We carried out an ANCOVA analysis and simple linear regressions on the available data, aiming to find solid morphometric relationships to convert some of our observations into units of measurement comparable with the variables used later in the equations.

The overall model, calibrated with records collected from a peach orchard in 2013, well simulated every variable of the tree we had observations of.

Results were good enough to implement an expansion of the model to make it able to predict the dynamics of the system in subsequent years. The lack of empirical data and theoretical interpretation of the physiological dynamics

taking place in this phase of the plant life forced us to adopt a discrete-time system of equations to initialize the tree at the beginning of each growth season. We had to summarize the phenological processes of the plant by linking the initial conditions of a year with the final values of the state variables at the end of the previous year: in particular, we investigated how the initial fruit and shoot bud onset is affected by the length of one-year-old shoots; then, we explored how the interaction between these mature shoots and temperature influences fruit and shoot initial average size.
We used the observed variables driving the transitions between years 2012-2013 and between years 2013-2014 to calibrate the additional parameters of the multiannual model, keeping measurements from the growth seasons in 2014 and 2015 for validation. Simulations of the available data were not completely satisfying, showing some divergences at the end of 2014 already and becoming wider in the prediction of the final state of the trees in 2015.

6.1 Open issues and future developments

We did manage to combine a quantitative description of the yield and a physiological description of the dynamics at the whole plant level in order to reproduce the growth and the nutrient partitioning of a deciduous fruit tree during a single season.
The model we developed could be used already to find how trees, and the crop production consequently, are immediately and directly affected by different agricultural practices. Not only by experimenting several combinations of pruning and thinning intensities, but, for example, by altering the frequency and the amount of fertilization applied and thus acting on the nitrogen net absorption rate parameter (paragraph 3.1.1). Simulating realistically the tree mechanistic behaviour, our model could enhance harvest optimization and exploitation.

However, data collected during more years could have allowed us to fully validate the continuous-time system and to test both our offline and online calibration. Understanding when and how fruit drop from the tree was made especially hard by the lack of solid theoretical sources: most of the literature we found came from the agricultural context, where the Ripening Loss in particular is usually neglected due to harvesting practices.
A larger window of observations would be needed to properly calibrate and validate also the multiannual version of the model. We already mentioned that we did find many knowledge gaps about storage dynamics in the literature, and this heavily limited us in deriving the relationships behind our multiannual model. Therefore, the simulations extended over multiple seasons did not meet our expectation.

Further research is required for a better understanding of how deciduous fruit trees accumulate, partition and then draw their reserves during the annual phenological cycle.
Including nutrient reserves as state variables could greatly improve the capacity of the model to describe the transitions before and after the dormancy period. In addiction to that, it would be possible to consider the dependency of some of the parameters of the continuous-time model from environmental and meteorological factors in order to simulate different scenarios of Climate Change affecting crop production and tree dynamics in the long run. For example, a deeper focus on the plant vegetative allocation parameter (paragraph 3.2.1) could lead to consider explicitly the role of temperatures and photoperiod in slowing down the shoot growth with the approach of autumn.
Other limiting substances as well, like phosphorus, could be added without modifying the main structure of the model if a more sophisticated and complex description is needed.
A further development might bring to couple our model with a model of

infesting pest population, which may lead to an interesting description of the interaction between the tree (and its fruits yield) and the pest dynamics.

Bibliography

Andersen, Peter and Bruce C. Schaffer. *Handbook of Environmental Physiology of Fruit Crops. volume I, Temperate Crops*. 1994 (cit. on p. 44).

B.G. Coombe. "The Develoment of Fleshy Fruits". In: *Annual Review of Plant Physiology* 27 (1976), pp. 207–228 (cit. on p. 29).

Bruchou, Claude and Michel Génard. "A space-time model of carbon translocation along a shoot bearing fruits". In: *Annals of Botany* 84 (1999), pp. 565–576 (cit. on p. 41).

Burnham, Kenneth P., David R. Anderson, and Kathryn P. Huyvaert. "AIC model selection and multimodel inference in behavioral ecology: Some background, observations, and comparisons". In: *Behavioral Ecology and Sociobiology* 65 (2011), pp. 23–35 (cit. on p. 39).

Estornell, Leandro H. et al. "Elucidating mechanisms underlying organ abscission". In: *Plant Science* 199-200 (2013), pp. 48–60 (cit. on p. 30).

Fishman and Génard. "A biophysical model of fruit growth: simulation of seasonal and diurnal dynamics of mass". In: *Plant, Cell and Environment* 21 (1998), pp. 739–752 (cit. on p. 1).

Génard, M. et al. "A simulation model of growth at the shoot-bearing fruit level. II. Test and effect of source and sink factors in the case of peach". In: *European Journal of Agronomy* 9 (1998), pp. 189–202 (cit. on p. 1).

Gillaspy, Glenda et al. "Fruits : A Developmental Perspective". In: *American Society of Plant Physiologists* 5 (1993), pp. 1439–1451 (cit. on p. 29).

Grossman and Theodore M. DeJong. *Maximum Fruit Growth Potential Following Resource Limitation During Peach Growth*. 1995 (cit. on p. 1).

Grossman, Y. L. and T. M. DeJong. "PEACH: A simulation model of reproductive and vegetative growth in peach trees". In: *Tree Physiology* 14 (1994), pp. 329–345 (cit. on pp. 33, 42, 49).

Hartmann, Henrik and Susan Trumbore. "Understanding the roles of nonstructural carbohydrates in forest trees - from what we can measure to what we want to know". In: *The New phytologist* 211 (2016), pp. 386–403 (cit. on pp. 45, 48).

Isagi, Y. et al. "How does masting happen and synchronize?" In: *Journal of Theoretical Biology* 187 (1997), pp. 231–239 (cit. on p. 45).

Schulze, E.-D., E. Beck, and K. Müller-Hohenstein. *Plant Ecology*. 2005 (cit. on pp. 2, 5).

Silva, David Da et al. "Modeling Seasonal Patterns of Carbohydrate Storage and Mobilization in Peach Trees". In: (2013), pp. 2006–2008 (cit. on p. 48).

Singh, Rajesh Kumar et al. "Photoperiod- and temperature-mediated control of phenology in trees – a molecular perspective". In: *New Phytologist* 213 (2017), pp. 511–524 (cit. on pp. 3, 4).

Stephenson, A G. "Flower and Fruit Abortion: Proximate Causes and Ultimate Functions". In: *Annual Review of Ecology and Systematics* 12 (1981), pp. 253–279 (cit. on pp. 29, 31, 35).

Symonds, Matthew R E and Adnan Moussalli. "A brief guide to model selection , multimodel inference and model averaging in behavioural ecology using Akaike ' s information criterion". In: *Behavioral Ecology and Sociobiology* 65 (2011), pp. 13–21 (cit. on p. 39).

Thornley, J. H. M. "A Balanced Quantitative Model for Root: Shoot Ratios in Vegetative Plants". In: *Annals of Botany* 36 (1972), pp. 431–441 (cit. on p. 26).

Thornley, John H.M. "Modelling shoot: Root relations: The only way forward?" In: *Annals of Botany* 81 (1998), pp. 165–171 (cit. on pp. v, vii, 2, 7, 23, 25, 27, 41, 42, 57).